FUGRO AIRBORNE SURVEYS PTY LTD

TECHNICAL REPORT
ON THE GEOLOGICAL INTERPRETATION OF AIRBORNE MAGNETIC AND RADIOMETRIC DATA, GRASSY, KING ISLAND

22nd May 2008

By: R. Miller and W. Crowe

TECHNICAL REPORT
ON THE GEOLOGICAL INTERPRETATION OF AIRBORNE MAGNETIC AND RADIOMETRIC DATA, GRASSY, KING ISLAND

Prepared for

KING ISLAND SCHEELITE LIMITED

Report prepared by: R. Miller and W. Crowe

Authorised for release by: H. Anderson ……..
Manager – Interpretation

Fugro Airborne Surveys Pty Ltd
65 Brockway Road, Floreat WA 6014, Australia
Tel: (61-8) 9273 6400 Fax (61-8) 9273 6466

Contents

Figures

Tables

EXECUTIVE SUMMARY

Interpretation of the airborne geophysical data has resulted in an integrated geological/geophysical interpretation of distinct units within the survey area. The interpretation has primarily utilised the aeromagnetic data to produce the pseudo-geological map, though radiometric, Landsat and DEM data were also incorporated.

The airborne data has enabled the geology surrounding the King Island Scheelite Mine to be refined from previous work. In addition, the interpretation of relatively recent regional geophysical data provides a better understanding of the geological evolution of King Island with regard to the relative timing and control of the major N – S trending faults with respect to the emplacement of the Devonian granites and the associated scheelite skarn mineralisation.

The possibility of further mineralisation in the area immediately adjacent to the existing mine workings has not been discounted. The geological interpretation suggests the presence of Mine Series rocks both to the east of Decline Fault, possibly to the contact with the Grassy River Fault, and to the south east of the open cut pit, beneath Grassy Bay. The presence of any interpreted 'Toredo' extension of the Dolphin orebody cannot be directly detected from the magnetic data which is consistent with the low magnetic susceptibility nature of the ore.

From the geological interpretation it is possible that the works associated with the proposed extension to the King Island Scheelite Mine may encounter a number of fault structures which may have implications for mining operations. Werner deconvolution modelling of the magnetic data provides an approximation of the depth to 'magnetic basement' in the area beneath the old sea dump and Grassy Bay. Results compare well with the limited drill log data available. The depth to basement increases quite rapidly across the old sea dump, from approximately 30m to over 60m indicating a localised increase in the overlying unconsolidated sediments or a fault structure with vertical offset. It should be noted that the depth to magnetic basement may not equate to the depth to consolidated material as non-magnetic sediments may overly the 'magnetic basement' being modelled.

1 INTRODUCTION

Fugro Airborne Surveys - Perth (FASP) was contracted by King Island Scheelite Limited to interpret airborne magnetic and radiometric data from Grassy, King Island. The location of the survey area is provided in Figure 1-1. The survey was flown during November 2007, and data processing was completed in mid- March 2008. The subsequent interpretation of the processed data is the subject of this report.

The objective of the geophysical interpretation was multi-fold. A geological interpretation of the solid geology was required to further assist the understanding of the area including the assessment of major faults and, locally the three dimensional orientation for some of these structures. The data were also examined for the presence of any extensions to the known mineralisation in the area. Modelling of the magnetic data also provided estimates for the depth to 'magnetic basement' underlying the sea, particularly beneath the old 'sea dump', was also undertaken.

Datasets acquire during the 2007/2008 airborne geophysical survey included magnetic, gamma-ray spectrometer (radiometric) and digital elevation data. Flight lines were oriented E-W (090°) at a spacing of 20m, tie lines oriented N-S (000°) at a spacing of 200m, and with a nominal terrain clearance of 20 - 30m. Magnetic field parameters at the centre of the project area are, total magnetic field intensity of 61219nT, field inclination of -70.8° and field declination of 12.1°.

Following a meeting between Robin Morritt of King Island Scheelite Limited and Fugro Airborne Surveys – Perth it was requested that open source magnetics and radiometric data be provided. This was to be incorporated with cultural data, such as roads, towns, place names and areas of previous investigation.

Open source regional data were downloaded from the Geoscience Australia website via the Geophysical Archive Data Delivery System. The airborne survey was flown and processed by Kevron Geophysics Pty Ltd on behalf of Mineral Resources Tasmania. The survey was flown between 15th and 21st January 2001 using a line spacing of 200m, tie line spacing of 2000m with a nominal terrain clearance of 80m.

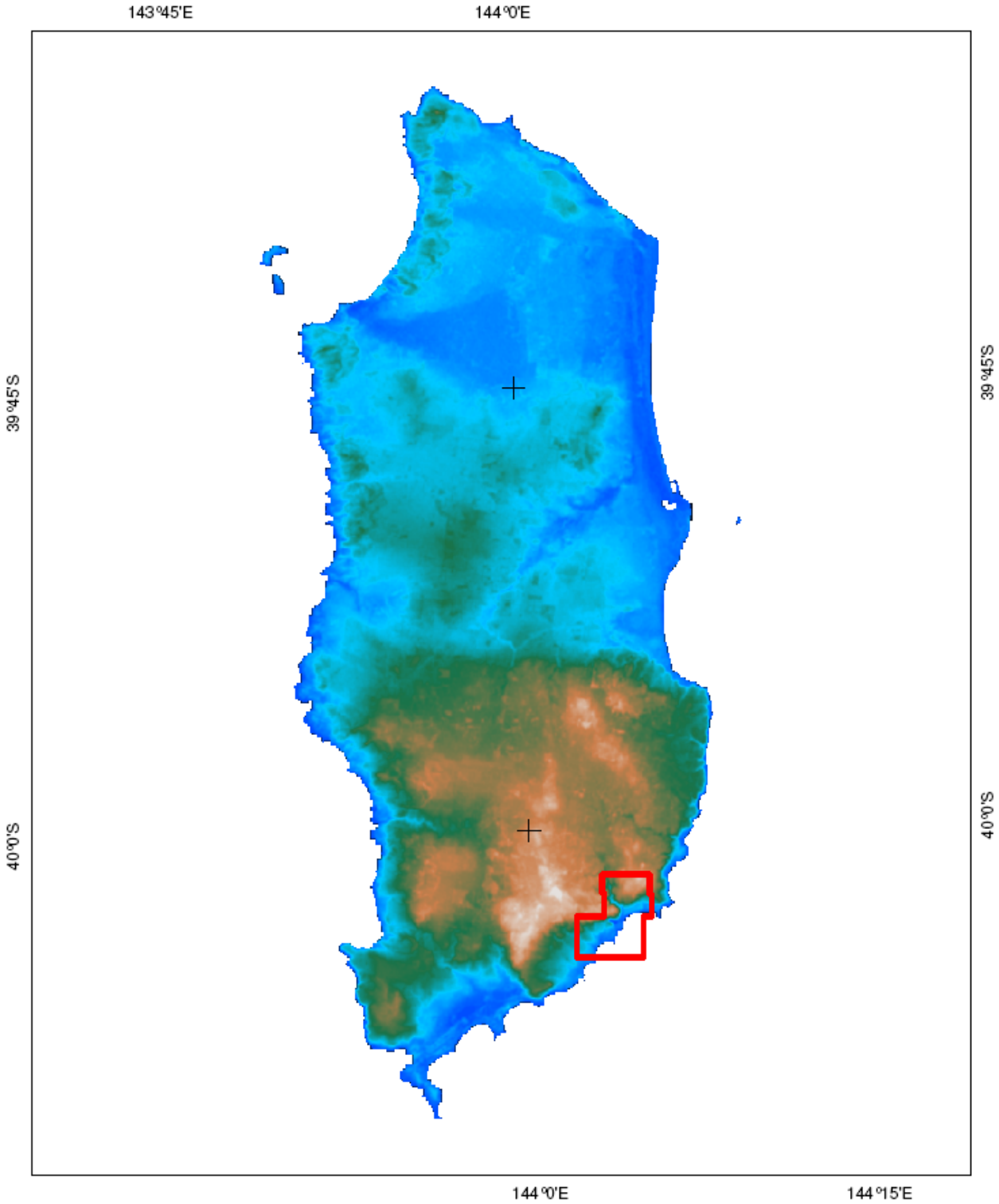

Figure 1-1: Location of the airborne geophysical survey (red outline).

Qualitative interpretation of the magnetic and radiometric data involved compilation of one 1:15,000 scale map product for the new data and one 1:150,000 scale map product covering the open source, regional data. The interpreted geology map results from the integration of the magnetic, radiometric and Landsat data and published/proprietary data.

Approximately 25 working days were assigned for interpretation, generation of specific processing products and reporting. The final products as displayed in this report include:

- A series of potential field (magnetic and radiometric) data map products.
- Solid geological interpretation map at 1:15,000 scale based on the airborne geophysical data, with explanation.
- Presentation of open source, regional data at 1:150,000.
- All data compiled into an ArcGIS GIS package.

2 REGIONAL GEOLOGICAL SETTING

King Island is located in Bass Strait, to the North West of Tasmania and midway between Tasmania and mainland Australia. The island measures approximately 65km in length and 25km in width and has very low relief, with the highest point being approximately 150m above sea level.

The geology of King Island consists primarily of Proterozoic rocks with late intrusion of Devonian granites (Figure 2-1). Extensive windblown Pleistocene to Recent sand cover extensive areas of the island with outcrop of basement lithologies limited primarily to the coastal fringe and along stream beds within the south-east (Gresham 1972). The western half of the island differs from the eastern half geologically and the relationship between the two halves is problematic. The majority of the island is underlain by a thick (13,000m +) sequence of variably metamorphosed Proterozoic marine sediments (Calver 2007).

Western King Island displays Mesoproterozoic (approximately 1300Ma) amphibolite-grade metasediments. These rocks have been regionally deformed and metamorphosed at approximately 1290Ma and were intruded by Neoproterozoic granites at approximately 760Ma.

The rocks of eastern King Island consist predominantly of a thick succession of relatively unmetamorphosed siltstones. It is probable that these siltstones correlate to the lower Neoproterozoic (approximately 1000 – 750Ma) Cowrie Siltstone of north-western Tasmania. The contact between these siltstones and the metasediments is concealed by surface cover and the nature of this contact (fault or unconformity), is unknown. Along the south-east coast an upper Cryogenian to Ediacaran succession of east dipping diamictite, cap dolostone, shale and mafic volcanic rocks (basalt and picrite) overly the siltstones.

Along the east coast, three small, early Carboniferous granite stocks intrude Neoproterozoic sediments. Scheelite ore bodies occur in the contact aureoles of the two southernmost stocks, the Grassy Granite and the Bold Head Granite.

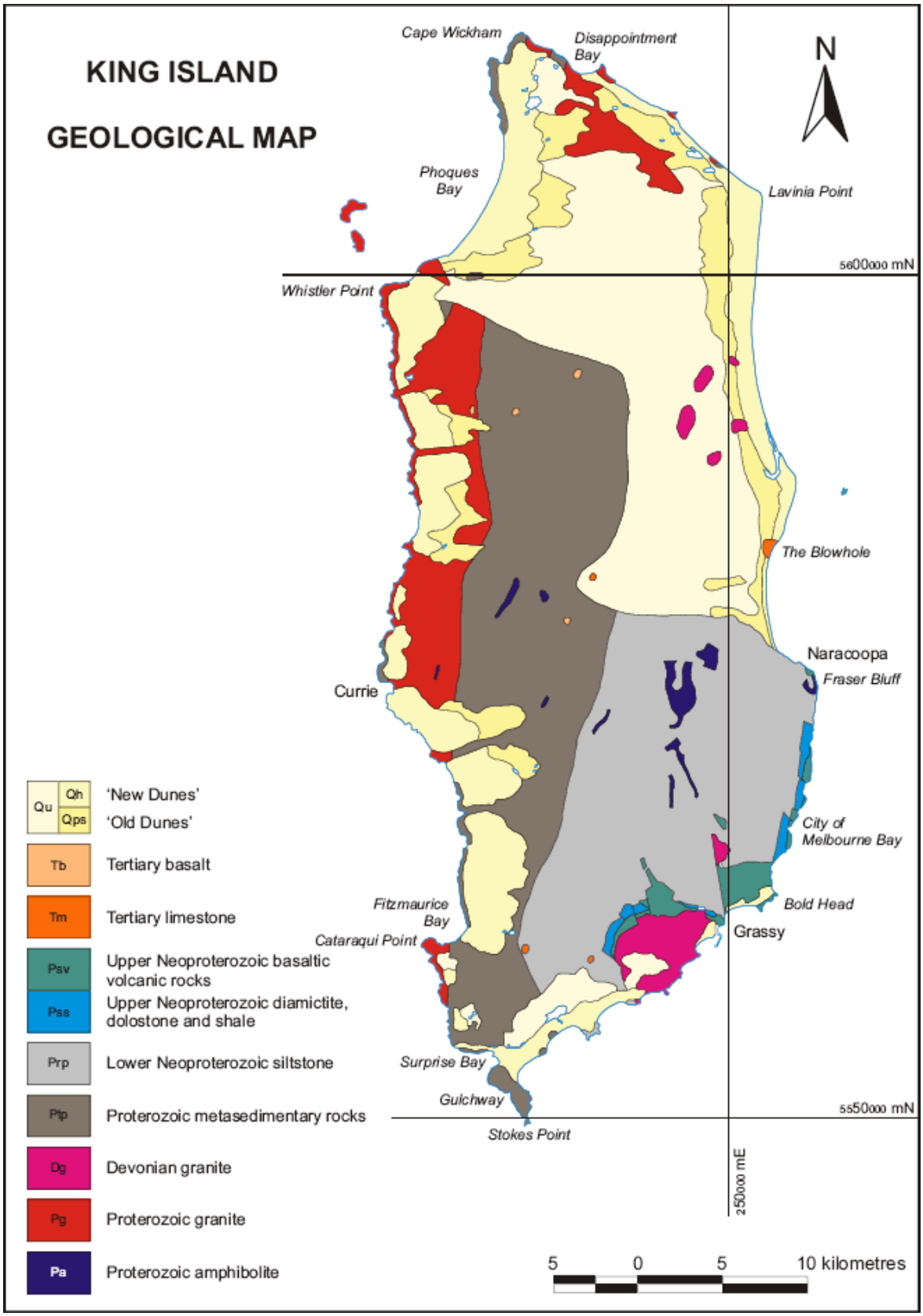

Figure 2-1: Geology of King Island (from Calver 2007*).*

2.1 WESTERN KING ISLAND

Western King Island is dominated by the metasediments of the Surprise Bay Formation (approximately 1300Ma) with minor mafic intrusives (Calver 2007). The metasediments consist of at least 1000m of primarily quartzfeldspathic schist, consisting typically of quartz, muscovite, biotite and plagioclase. Minor quartzite, pelitic schist and rare calcareous lenses are also present. The mafic intrusives are amphibolites with a chemical composition similar to tholeiitic basalt (Calver 2007).

Zircons within a sample of turbidites to the north of Fitzmaurice Bay provide a maximum constraint for the depositional age of the Surprise Bay Formation (Calver 2007). The youngest age from detrital zircons is approximately 1350Ma with a predominance of ages around 1450Ma and 1600 - 1850Ma.

Dating of metamorphic monazite by electron microprobe from metasediments at Fitzmaurice Bay and Surprise Bay, located some distance from the granite aureoles present, provides ages of approximately 1270Ma (Calver 2007: Figure 2-2). This age has been interpreted as the age of the regional deformation resulting in the amphibolite-grade metamorphism of the metasediments (Calver 2007). This metamorphic event is unknown elsewhere in north-west Tasmania. Here the Rocky Cape Group, which is considered to be the oldest succession, has been aged significantly younger at <1000Ma (Figure 2-2). Elsewhere, the Franklin Metamorphic Complex in Central Tasmania, which is the only known occurrence of possible Mesoproterozoic basement on mainland Tasmania, does record an event at 1300Ma in monazite in the cores of garnets (Calver 2007).

Early work identified the early phase of regional metamorphism as being related to the west coast granitoids, resulting in all the events being included in the Wickham Orogeny at approximately 760Ma (Cox 1989; Turner et al. 1998). Dating of the early regional phase at 1270Ma (Berry et al., 2005) means that at the present time the Wickham Orogeny includes only the granitoid intrusions and associated deformation in the aureoles (Figure 2-2). This interpretation is consistent with the lack of evidence for an orogeny at 760Ma in mainland Tasmania or southern Australia.

Within the margin of the pluton east of Cape Wickham on the northern tip of King Island are cross-cutting relationships, indicating major granitic intrusive activity post-dates the event at 1270Ma discussed above. The most dominant, and earliest, intrusive rocks are S-type, K-feldspar porphyritic biotite adamellite whilst later, minor associated intrusives include S-type biotite granodiorite, even-grained biotite adamellite, biotite-muscovite granite, aplite and

pegmatite. The most recent dating of these rocks using SHRIMP Pb-Pb on zircon has provided dates of 760 +/- 12Ma from samples from Cape Wickham and 748 +/- 2Ma from samples taken near Currie (Turner et al. 1998; Black et al. 1997: Figure 2-2).

2.2 EASTERN KING ISLAND

Underlying the eastern half of King Island is a 6 – 7km thick succession of relatively unmetamorphosed shale, siltstone and fine-grained muscovite quartz sandstone dipping and facing the east, designated the Naracoopa Formation. Lithologically, the Naracoopa Formation is similar to the Cowrie Siltstone found in north-west Tasmania, part of the Rocky Cape Group which has a depositional age of between 750 and 1000Ma. The detrital zircon age distribution of the unit is similar to the Rocky Cape Group and Oonah Formation of western Tasmania (Black et al 2004: Figure 2-2). Surficial sediments cover the contact between the Surprise Bay Formation of western Tasmania and the Naracoopa Formation. Therefore it is unclear whether the contact is a fault, unconformity or metamorphic transition.

Along the south-east coast the Grassy Group, a late Neoproterozoic succession of diamictite, dolomite, limestone, shale and mafic volcanics (basalt and picrite), overlies the Naracoopa Formation. As with the major east - west boundary, the contact between the Naracoopa Formation and the Grassy Group is poorly exposed and unclear, either regionally conformable or unconformable.

Should the shale-siltstone unit correlate with the Rocky Cape Group, which has an age of greater than 750Ma, then there must be a significant lacuna present as the Grassy Group is probably younger than 650Ma. It is possible that the Grassy Group may correlate with the Success Creek Group which is found on mainland Tasmania (King Island Scheelite Ltd 2006). An unconformity within the Grassy Group at this level might correspond to the Wickham Orogeny of western King Island.

Within the Grassy Group a succession of mafic rift volcanics is present approximately 100m above the top of a Marinoan glacial correlative. This is similar to successions observed in parts of southeastern Australia and Tasmania where late Neoproterozoic sedimentation was interrupted by the extrusion of mafic rift volcanics associated with development of a volcanic passive margin (Crawford et al 1997; Calver and Walter 2000; Direen and Crawford 2003; Meffre et al. 2004).

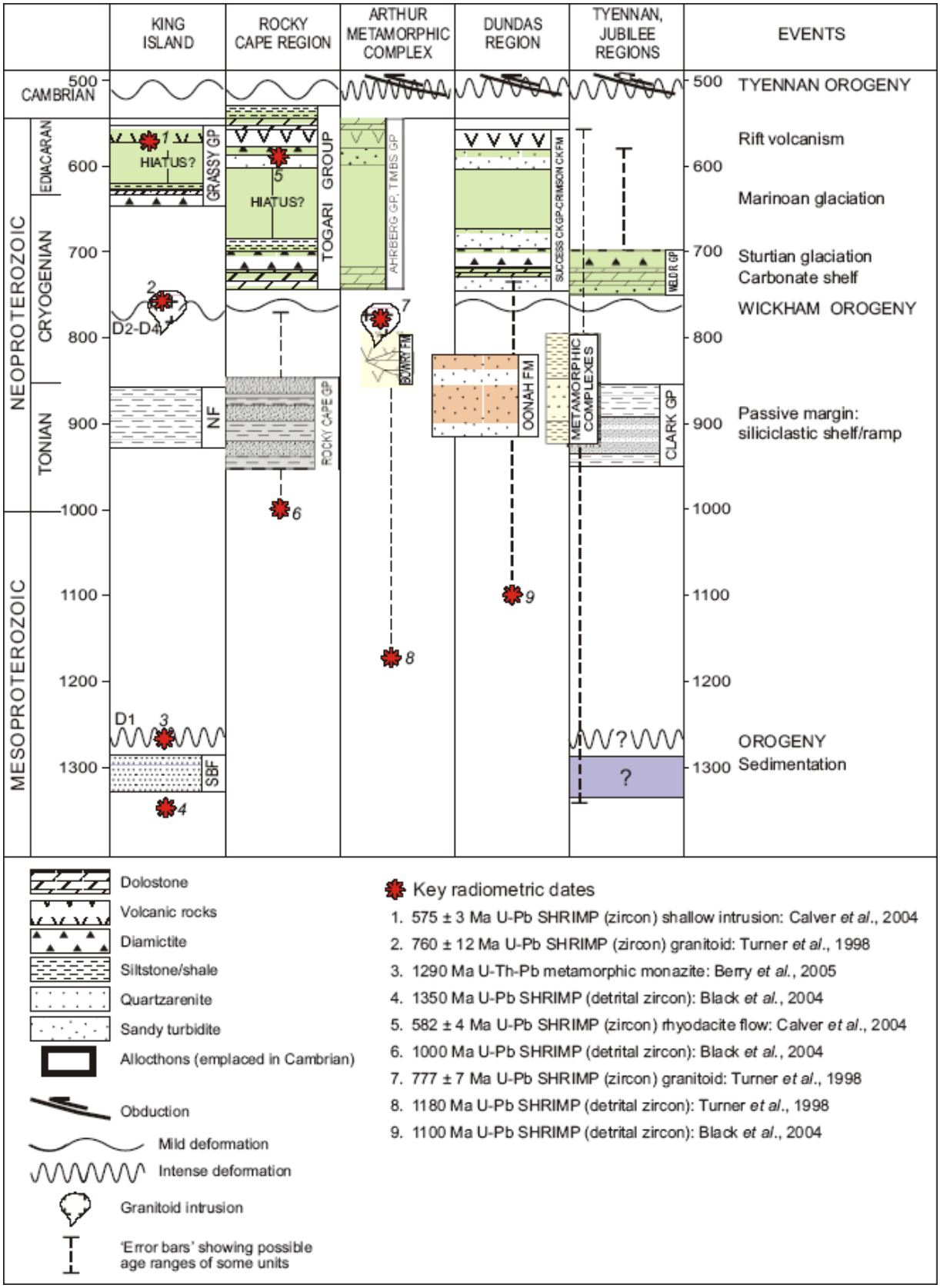

Figure 2-2: Time space diagram for Proterozoic of King Island and other Tasmanian terranes (from Calver 2007).

Along the southeast coast of King Island, around City of Melbourne Bay, the Grassy Group is well exposed and can be seen to dip and face towards the east. From its base the group can be seen to consist of (Calver 2007):

Cottons Breccia – approximately 100m of predominantly pebble to boulder grade diamictite with clasts of fine-grained quartzite, siltstone and shale. These are similar to the underlying succession but also include carbonate, chert, rare basalt and other lithologies which are not present. In the middle of the succession is a tuffaceous sandstone up to 10m thick, possibly originally of mafic composition but now altered to carbonate and chlorite. Dating of the top of this unit using detrital zircon results in a population of ages clustered around 655 – 635Ma.

Cumberland Creek Dolostone – a 10m thick band of pale pinkish-grey, fine-grained, laminated dolostone that passes up into thinly interbedded dolostone, limestone and shale. This thin unit displays a distinctive lithology and ^{13}C-depleted, upward decreasing carbon isotope signature that matches that of the Nuccaleena Formation, a widespread 'cap dolostone' found to overlie Marinoan glacials on mainland Australia.

Yarra Creek Shale – planar-laminated shale displaying occasional thin, graded beds of volcaniclastic sandstone. In the middle part of this unit are black shale beds possessing sedimentological characteristics of fossil benthic microbial mats. This provides further evidence of correlation with units on mainland Australia as this type of shale is locally present in post-glacial successions.

Grimes Intrusive Suite – differentiated sills intruded above the three units previously mentioned. They are generally andesitic in composition with fractional crystallisation in situ post-intrusion has resulted in a zone of pyroxene-rich gabbro at the base. The sills have an unusual composition in that the upper and middle parts are approximately 55 – 65% SiO_2 but with abnormally high MgO, Cr and Ni content, indicating a mafic source. Evidence for crustal contamination is provided by anomalies in Nd isotopes and trace elements. Even though the sills are locally vesicular, suggesting shallow intrusion, the Yarra Creek Shale would appear to be at least partially lithified prior to intrusion. SHRIMP U/Pb dating on zircons from these intrusives revealed an age of 575 +/- 3Ma.

City of Melbourne Volcanics – consists of a thickness of up to 100m of tholeiitic pillow lavas, peperites and volcaniclastic sandstone. There is evidence of extrusion of this unit into soft sediments at the top of the Yarra Creek Shale by the presence of peperites, hyaloclastite breccias and lobate intrusions with a matrix of baked mudstone. As with the Grimes Intrusive Suite the Nd isotope composition indicates crustal contamination, but not to the same extent.

Shower Droplet Volcanics – picritic interbedded pillow lavas, thin flows and hyaloclastites approximately 200 – 300m displaying characteristically high MgO and very low incompatible element concentrations. This unit is thought to disconformably overlie the City of Melbourne Volcanics.

Bold Head Volcanics – more than a 300m thickness of tholeiitic basalt flows, pillow lavas and volcaniclastic sandstone and conglomerate, compositionally similar to enriched mid-ocean ridge basalts. Although there is no observable stratigraphic contact with the underlying rocks dykes of similar composition to the Bold Head Volcanics cut both the City of Melbourne Volcanics and the Shower Droplet Volcanics. Both the Shower Droplet Volcanics and the Bold Head Volcanics have a Nd-Sm isochron age of 579 +/- 16Ma.

These three volcanic units have been termed the Skipworth Subgroup by Meffre et al (2004).

Although the top of the volcanic succession is not exposed and lies offshore beneath the Tasman Strait, a total thickness of 8500m of mafic volcanic rocks has been calculated from modelling of aeromagnetic data. The lithology of the overlying succession is unknown but in northwest Tasmania the Smithton Dolomite conformably overlies the Kanunnah Subgroup, which is compositionally similar though much thinner than the volcanic succession on King Island. A rhyodacite flow within the Kanunnah Subgroup has been dated at 582 +/- 4Ma whilst strontium isotope chemostratigrahpy dates the Smithton Dolomite at approximately 570 – 545Ma.

The Proterozoic sedimentary rocks of Eastern King Island have been intruded by three early Carboniferous granite bodies, the Grassy, Bold Head and Sea Elephant plutons, of which Sea Elephant is the largest. All three intrusions are classified as monzogranite-granodiorite and are I-type.

Both the Grassy and Bold Head granodiorites average 68.5% SiO_2. They are porphyritic with large pink K-feldspar phenocrysts and their mineralogy consists of quartz, K-feldspar, plagioclase, biotite and amphibole. Minor apatite, alanite, sphene, magnetite and zircon are also present. Located on the east coast to the north of the Grassy and Bold Head plutons, the Sea Elephant pluton is an adamellite, considered to be the fractional equivalent of the two granodiorite intrusions. Sea Elephant is more felsic, at 70.15%, but texturally similar to the other two intrusions. It differs only in that it contains minor amounts of amphibole and sphene.

2.3 KING ISLAND GRANITOIDS – REGIONAL GRAVITY

Studies of the regional gravity field over King Island suggest that the bulk of the island is underlain by granitoids at depths ranging from 600 – 1600m (Leaman 2003). The Early-Carboniferous plutons appear to have intruded the Precambrian bodies of the western half of the island. Here gravity models agree with the exposed geology in that the dominant Precambrian rock-type is adamellitic (density of 2.65t/m^3 or less) with granodiorite (density of 2.69 – 2.71t/m^3) more prevalent in the central west.

The data indicates a number of individual plutons being present. The Grassy and Bold Head intrusions are much smaller than the Sea Elephant intrusion, with the majority of the volume of the Grassy pluton being at depth. Original modelling of the gravity data across the Grassy Granodiorite using a density of 2.70 – 2.71t/m^3 suggested a relatively insignificant volume of material being present. Leaman (2003) suggests from the gravity modelling that the greater part of the volume of the Grassy Granite at depth is a very siliceous granite with a reduced density of 2.60 – 2.62t/m^3 and that there is minimal granodiorite present. This implies that the granodiorite has been intruded by another adamellite/granite.

2.4 GRASSY SCHEELITE DEPOSIT

The Grassy scheelite deposit was discovered in 1904 by a prospector named Tom Farrell. Although completely covered by sand Farrell traced a scheelite-bearing formation in a fault (No. 3 Fault) inland from an outcrop exposed on the beach at the low water mark. The deposit is a large pyrometasomatic orebody formed by the selective replacement of limestone beds (Knight and Nye 1957).

Intermittent mining of the deposit was undertaken between 1917 and 1942 when a major geological survey and drilling programme confirmed the presence of a significant orebody. The mining operations were expanded and continued almost continuously until 1990 until prolonged depressed tungsten prices forced the mines closure. All mining infrastructure was removed at this point (King Island Scheelite Ltd 2006).

The intrusion of the Grassy and Bold Head granites resulted in extensive contact metamorphism of the sediments in the lower Grassy Group. These metamorphosed sediments are termed the ‘Mine Series’ (Gresham 1972). Original limestone beds were converted to marble, impure limestone or impure dolomitic limestone were converted to diopside-grossularite hornfels; calcareous shales became actinolite-biotite-feldspar hornfels; and shales were converted to biotite hornfels. Within the uppermost and lowermost beds of the Mine Series are forsterite-

phlogopite-spinel hornblende or tremolite rocks which may represent metamorphosed ultrabasic lavas or pyroclastics (Figure 2-3). It is known from both mapping and limited diamond drilling that the Mine Series rocks continue to the east along the southern boundary of the Bold Head Granite and to the west for about 5 kilometres around the Grassy Granite contact (Gresham 1972).

The host Mine Series sequence, as given by Calver (2007), in descending stratigraphic order is:

- B Lens hangingwall, hornfels, 10 – 20m thick; actinolite-biotite and biotite hornfels
- B Lens, 25 – 30m thick; banded sequence of biotite pyroxene hornfels, marble, grossularite with variable scheelite
- Hangingwall hornfels 5 – 50m thick; actinolite-biotite and biotite hornfels
- Pyroxene garnet hornfels, 2 – 15m thick; diopside and grossularite hornfels, calcite ovoids up to 150mm diameter, variable scheelite
- Upper C Lens, 0 – 20m thick, principal ore horizon; andradite skarn, marble, minor pyroxene-grossularite hornfels
- Marble marker, 1 – 5m thick; barren or weakly mineralised marble and pyroxene-grossularite hornfels, variable scheelite
- Biotite pyroxene hornfels, 20 – 30m thick; thinly banded (5 – 10mm) biotite-pyroxene-actinolite hornfels
- Lower metavolcanics, 5 – 8m thick; tremolite-phlogopite chlorite-magnetite rock

Metasomatism of marble beds within B Lens and C Lens has resulted in the conversion of the marble to skarn composed of andradite with interstitial quartz and minor pyroxene, actinolite, epidote, zoisite and scheelite. Small amounts of sulphides are also present. Fine-grained scheelite is present throughout the skarn with most formed as inclusions in, and adjacent to the margins of, andradite garnets. Some is also found in the interstitial quartz whilst coarser-grained scheelite can be found in the pyroxene garnet hornfels above C Lens and additionally in joint planes and quartz-filled tension gashes (Knight and Nye 1957; Calver 2007).

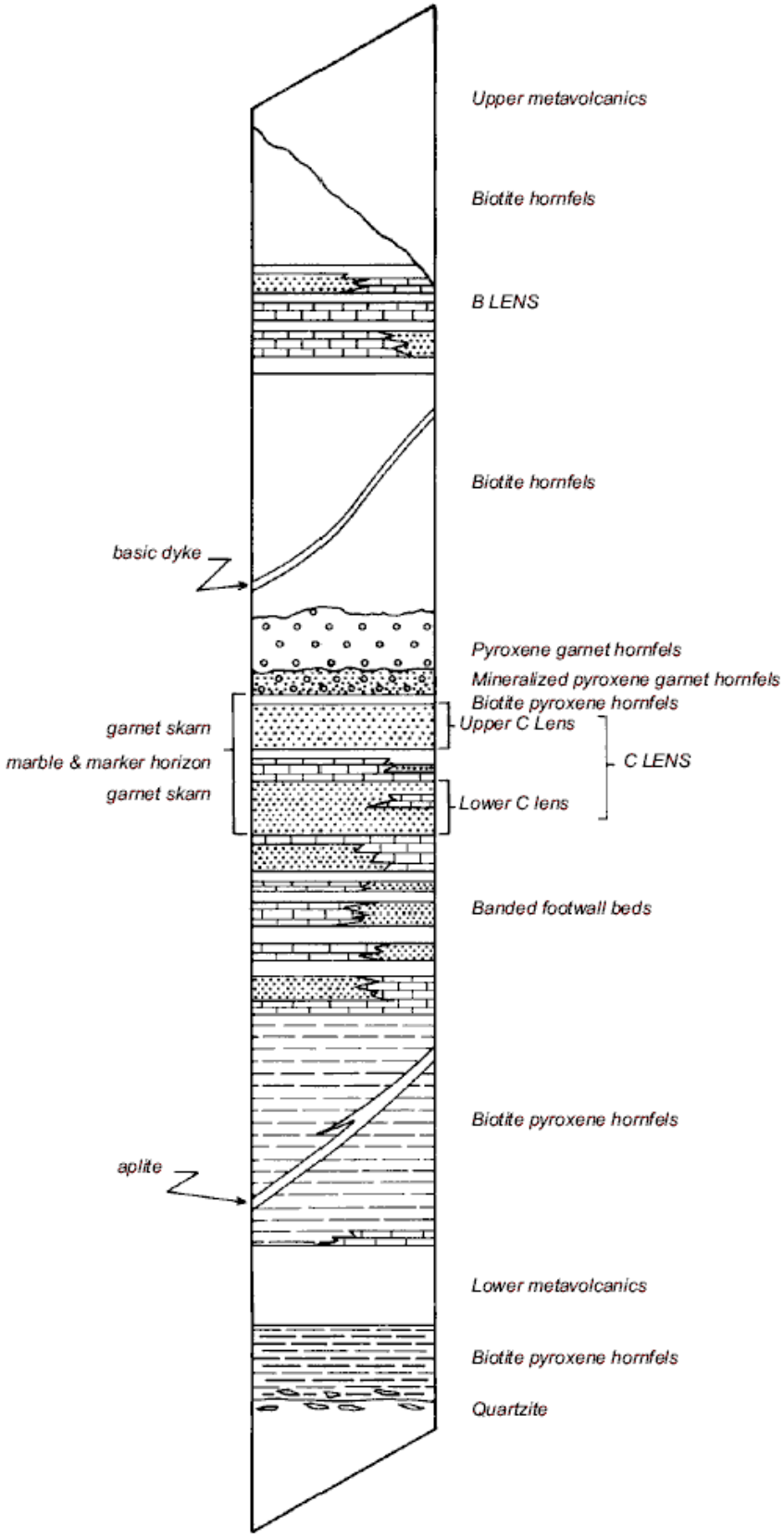

Figure 2-3: Stratigraphic succession, No. 1 Open Cut and Dolphin Mine (from Calver 2007).

Molybdenum enrichment of the primary scheelite occurs with the equivalent of approximately 30% powellite. Also found is some secondary molybdenum-poor scheelite which is usually associated with molybdenite. Small amounts of late-stage sulphides present within the ore include pyrite, pyrrhotite, arsenopyrite and chalcopyrite with minor sphalerite, galena, bournonite and bismuthinite near major faults.

Although distributed erratically, the scheelite is focussed within the B-Lens and C-Lens skarns. The grade tends to increase towards major faults indicating the hydrothermal fluids were able to ascend through the faulted pathways and then permeate through the reactive marble. It is considered by most workers that the mineralising fluids originated from an adjacent or underlying granitoid.

Generally all of the hornfels are barren and unaffected by the metasomatism except in small portions along fractures where slight replacement occurs. It appears that the metasomatism travelled along marble beds but not across the bedding, unless tension fractures are present. Within the C-Lens thin beds of marble are altered to andradite skarn. In contrast, identical beds above and below remain barren and unaltered, inert and impervious pyroxene-grossularite hornfels less than 30mm thick shielding them from the metasomatism.

It is common for beds of skarn to abruptly end against a minor fracture, possibly containing a film of quartz. The bed may have been displaced by the fracture, by as little as 10mm, but beyond it continues as unaltered marble.

The basic orebody structure is that of an anticlinal nose plunging south-east at approximately 30^{o}. The structure strikes at approximately 290^{o} with a dip of 15 – 20^{o} in the mined area and steepening down dip at the eastern end to 55 – 60^{o}. Further to the west the general dip is 30 – 40^{o}.

Structurally, the area is dominated by the east - west trending North Boundary Fault, No. 3 Fault (possibly a fault displaced extension of the North Boundary Fault), Swan Fault, Central Fault and Decline Fault. The North Boundary Fault terminates the skarn hosts in the north, whilst the skarn deposits are internally disrupted by the Swan, Central and Decline Faults. The north - west trending, southwest dipping, reverse Wedge Fault may have formed as a result of dilation during cooling of the granite.

Brown and Potter (1980) suggest three periods of faulting in the mine area (Figure 2-4):

1. East - west trending faults (eg. No. 3, Central and Swan Faults).

2. A series of northwest to southeast trending faults (eg. Wedge, Penguin and Pheasant).

3. Decline and possibly the Grassy River Fault, though there is insufficient evidence to be certain that the Grassy River Fault developed at this stage.

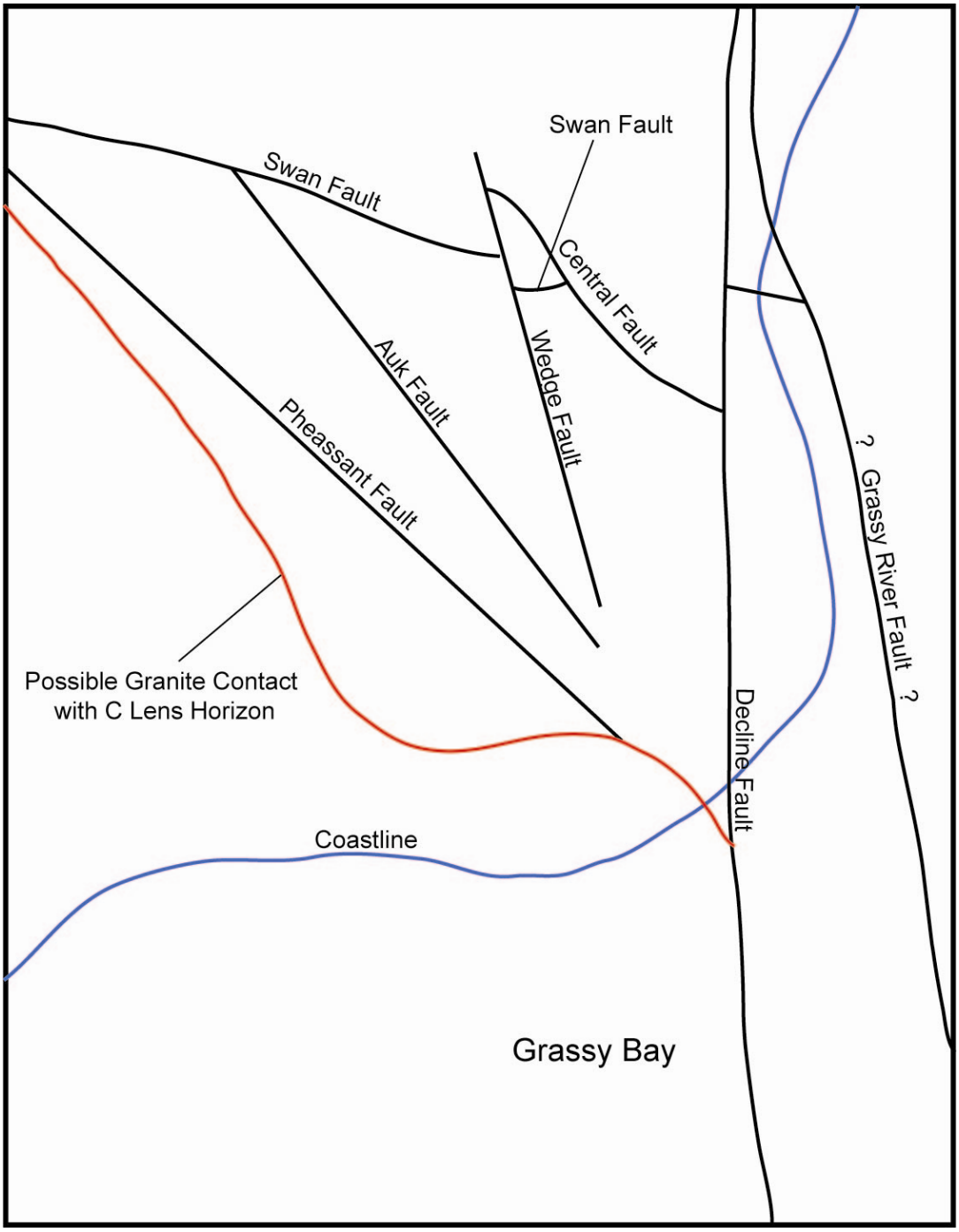

Figure 2-4: Detailed fault structure of Grassy Scheelite Deposit (from Parkes and Brown 1985*).*

Further to the east, the regional north trending Grassy River Fault terminates the skarns. Calver (2007) suggests the Bold Head Granite may be a faulted sliver of the larger Grassy Granite,

displaced along this structure to the north, whereas Gresham (1972) notes that the two intrusions have different magnetic characters, concluding they could not possibly be part of the same body. From the information available it is unclear as to whether the Grassy River Fault is an older structure that predates the granite intrusion or a younger post-intrusion feature.

Tectonism accompanying the granitic intrusion that resulted in large amounts of small-scale faulting and folding of the sediments. Two southeasterly plunging anticlines, one of which is visible in the open cut, provide the best ore development within their hinge zones. The ore bodies are relatively narrow and mineralisation is weaker within the intervening syncline.

3 AIRBORNE GEOPHYSICAL DATA

The high-resolution airborne geophysical data has been interpreted to identify lithomagnetic domains, structural trends, faults, fractures and folding. In addition, the open source geophysical data has been interpreted to provide an insight into the regional geological setting.

Integration of radiometric and magnetic data with the published geological data has allowed the construction of a lithostructural interpretation. All data have been rectified and projected in GDA 1994, MGA Zone 55.

3.1 MAGNETICS

A number of images of the magnetic data have been utilised during the interpretation process. The images found to be most useful were the Total Magnetic Intensity (TMI) Reduced to Pole image and the First Vertical Derivative (1VD) of the Total Magnetic Intensity Reduced to Pole. The following is a complete list of the magnetic images used for this project:

- TMI
- TMI Reduced to Pole
- First and Second Vertical Derivatives of the TMI Reduced to Pole
- Analytic Signal of TMI Reduced to Pole
- TMI Reduced to Pole, Upward Continued by 20m
- Each of the images, apart from the vertical derivatives, had a sunshade applied for presentational purposes.

Many of these processes can be carried out through either Fourier (Frequency) or Spatial filtering. For the Grassy survey area the Fourier transform technique of filtering was used. Fourier transform expresses a magnetic field as a set of sine and/or cosine waves of specific frequency, amplitude and phase.

The **Reduction to Pole (RTP)** filtering process was applied to gridded Total Magnetic Intensity (TMI) data. RTP is a well established numerical process (Baranov 1957) which transforms the inclination of the apparent magnetisation vector from that of the ambient field to that which exists at the magnetic pole (i.e. Inclination(I) = 90°). This has the effect of transforming dipolar

magnetic anomalies to monopolar anomalies centred over their causative bodies as shown in Figure 3-1.

Assuming magnetisation by induction, at the magnetic pole the anomaly shape is a symmetrical positive anomaly with the anomaly peak located directly over the centre of the source. At mid-magnetic latitudes the anomaly shape is distinctly dipolar and the centre of the source is located between the positive and negative peaks. At the equator the anomaly is a magnetic low centred directly over the centre of the source. See Figure 3-2 which shows the TMI grid in comparison with a TMI reduced to pole grid.

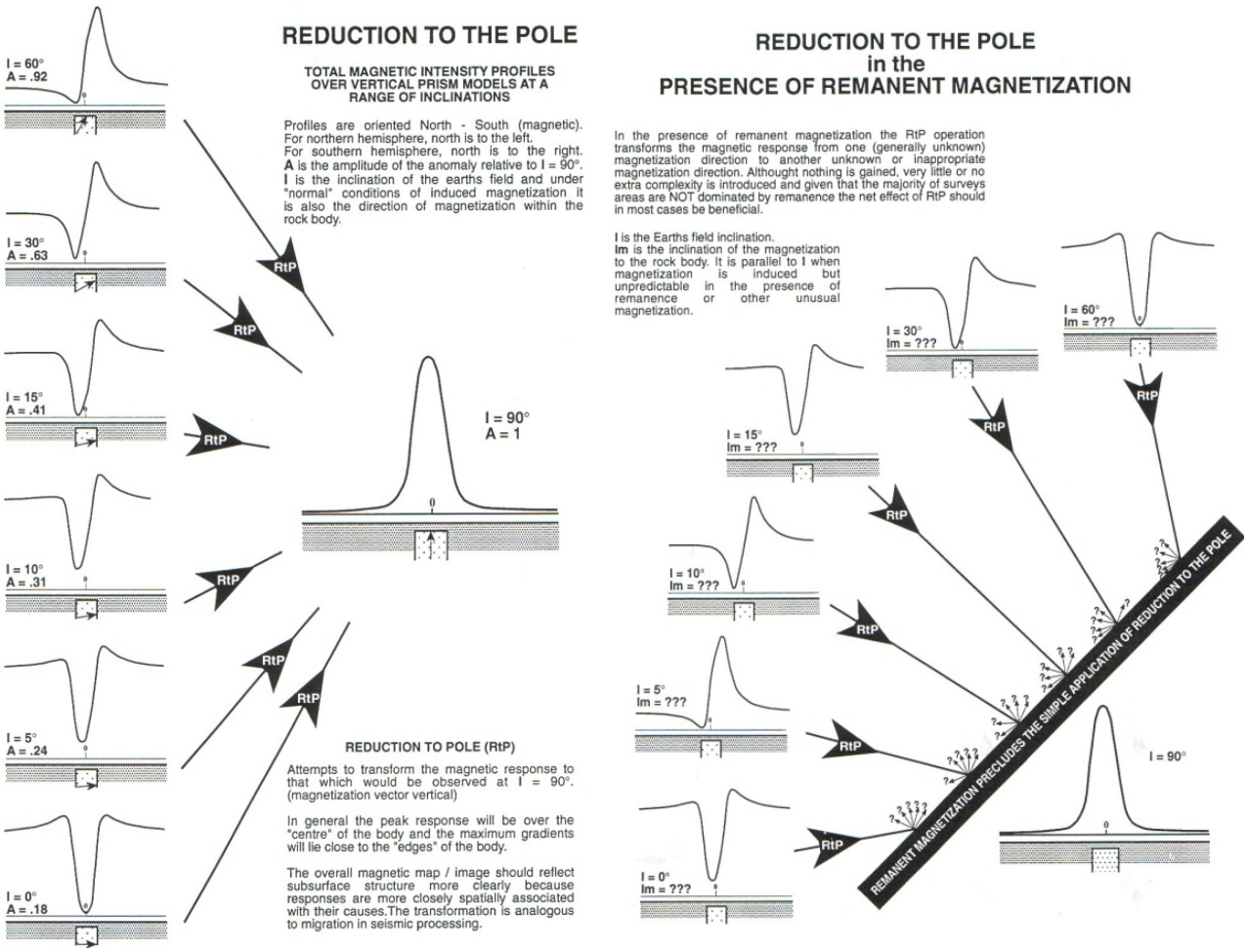

Figure 3-1: Examples of magnetic curves at different inclinations being subjected to reduction to the pole. Examples on the left are for normal induced magnetisation, and on the right with remanent magnetisation.

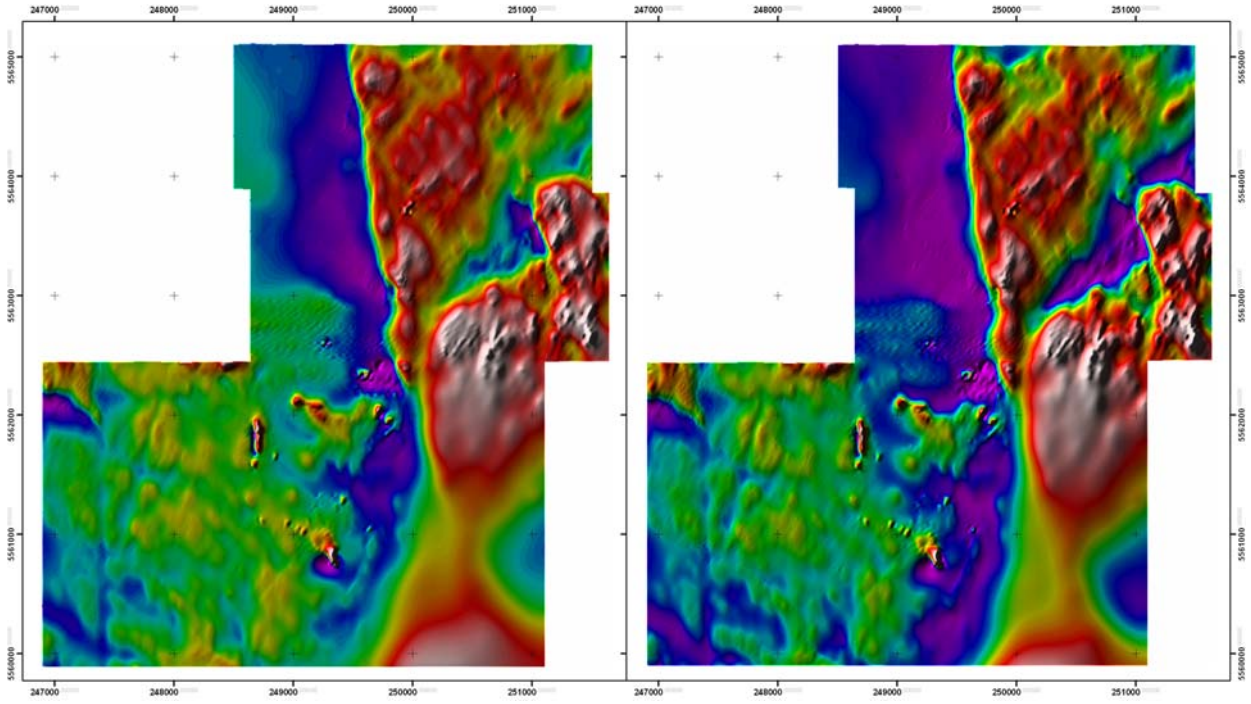

Figure 3-2: Pseudo colour image of the TMI grid (a) compared with a pseudo colour image of the TMI grid which has been Reduced to Pole (b). Note the south shift in anomalies and the better resolution of magnetic features.

Vertical Derivative filters were applied to the grid of the TMI (RTP) data. The **First Vertical Derivative (1VD)** of a magnetic field is an approximation of the field's instantaneous rate of change in the vertical direction. The function can be calculated in either the Fourier (frequency) or spatial domain (Figure 3-3). Calculating the 1VD in the Fourier domain is theoretically best as the entire grid is used in the computations, and thus biasing of an anomaly due to its wavelength is removed and the low-frequency component is maintained.

As the 1VD filter enhances high-frequency variations of the magnetic field, it is particularly useful for structural mapping through the definition of near-surface litho-magnetic boundaries and texture. Cosmetically, the 1VD appears to produce a sharper image of TMI or RTP data, in which boundaries are much better defined (Figure 3-4).

The **Second Vertical Derivative (2VD)** grid is approximately a 1VD of a 1VD enhancement. It further enhances features with very high spatial frequency. This filter is used in a similar way to the 1VD, and can be very useful for defining geomagnetic contacts. However, for the Grassy project the 2VD grid displays quite elevated noise levels, phenomena pointed out by Gunn et al.

(1997) who suggested that the second derivative can emphasise noise in the data to the extent that its superior resolution is negated.

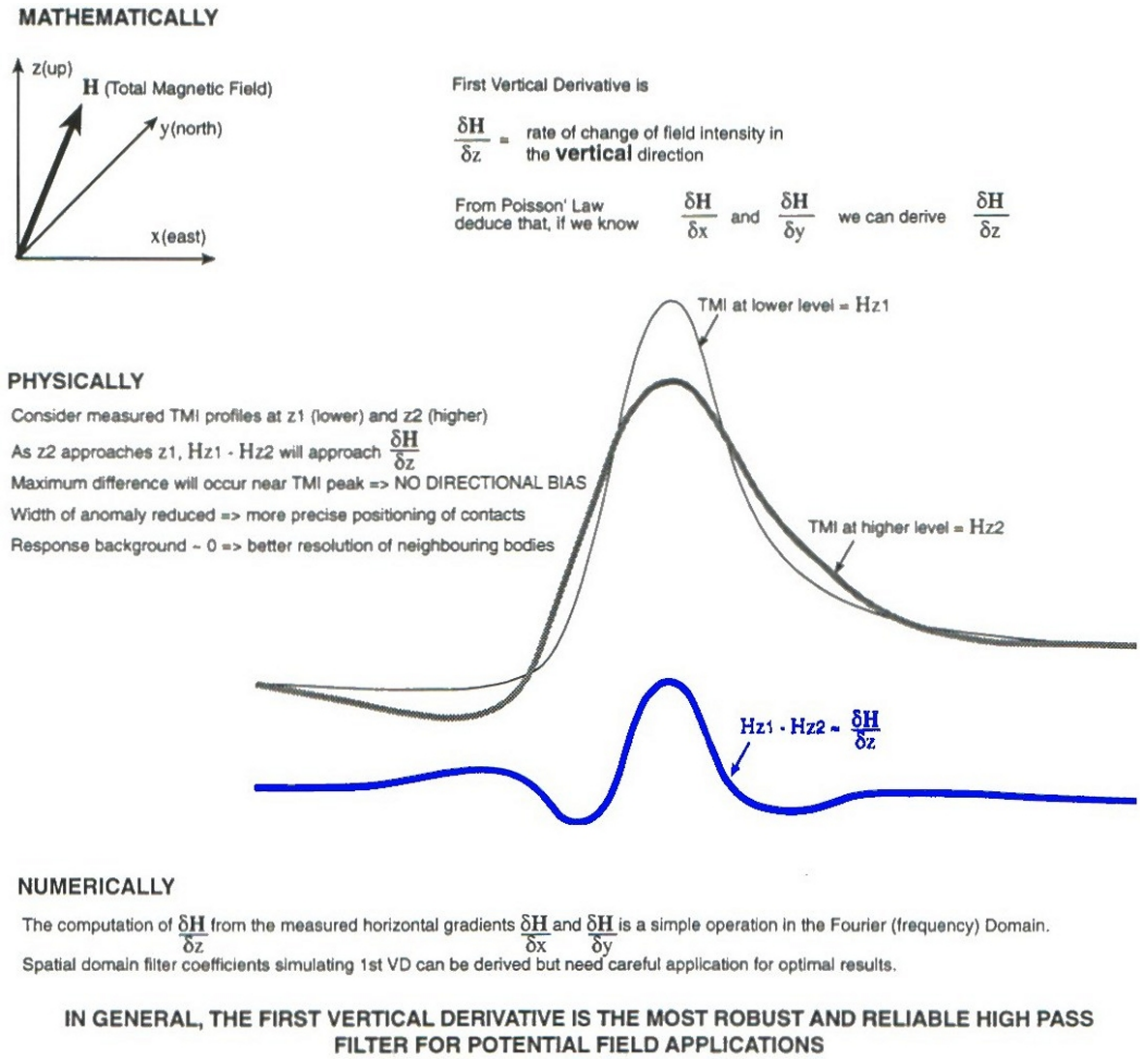

Figure 3-3: Schematic representation of the first vertical derivative (1VD).

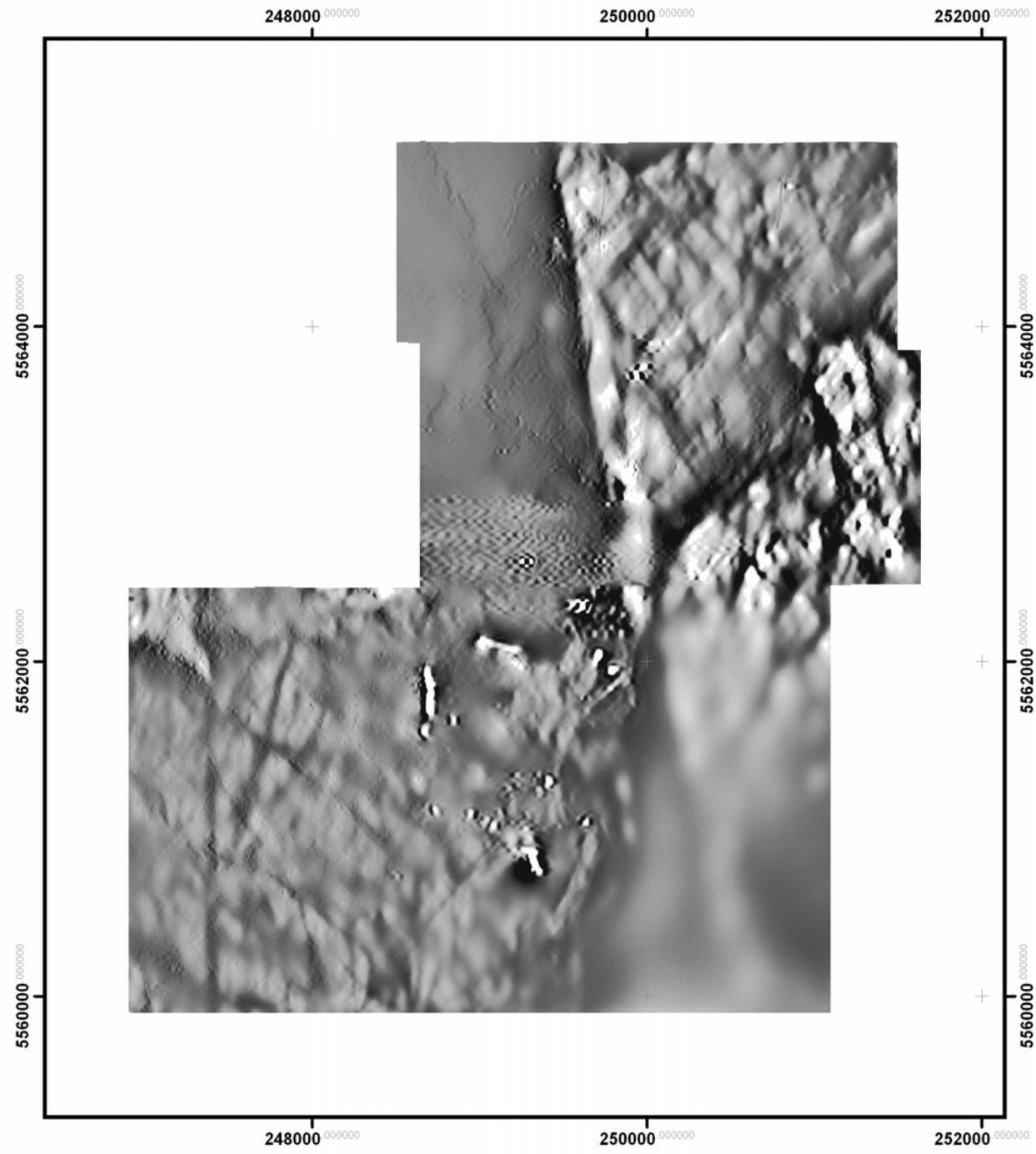

Figure 3-4: Greyscale image of the First Vertical Derivative of the TMI Reduced to Pole grid.

The **Analytic Signal (AS)** is the linear combination of the First Vertical and the First Horizontal Derivatives (Nabighian 1972). Various geological geometries have characteristic Analytic Signal curves; thin dykes have a single bell-shaped curve amplitude function with the peak over the centre of the dyke; thick dykes produce two peaks, one over each contact. For any arbitrary 2D body of polygonal outline, each corner contributes a bell-shaped curve segment. For a sub-

linear contact between two bodies, the amplitude of the Analytic Signal is a bell-shaped curve with peak amplitude directly over the contact. The amplitude function can be used directly in an interpretation scheme. It has a maximum value immediately above the contact and the depth to the contact can be calculated from the half-width of the symmetrical peak.

The analytic signal filter transforms both positive and negative anomalies into positive bell-shaped anomalies with the peaks located directly above contacts or centres of dykes, but makes no assumptions about the direction of magnetisation. If magnetisation were purely by induction, there should be a high degree of correlation between the vertically integrated 3D analytic signal amplitude and the RTP data. In areas of remanence the analytic signal and TMI grids will possess opposite sign.

Upward Continuation is the process of transforming potential-field data measured on one surface to some other higher surface, effectively taking the plane of measurement away from the sources. It is often used to reduce or minimise the effects of shallow sources or noise in grids and is considered to be a 'clean' filter as it produces almost no side effects that might require the application of other filters or processes to correct.

3.2 RADIOMETRICS

Gamma-ray spectrometer data are presented either individually as single element abundances for Potassium, Uranium, Thorium, as Total Counts or combined as a Ternary colour image with potassium (red), uranium (blue) and thorium (green). Combined radiometric images are very useful in displaying variation of these radioelements due to the influence of host lithology.

Gamma-ray data relate directly to surface units, whether exposed lithologies, shallow subcrop, surficial sediments or regolith, and reflect only on approximately the top 0.3 m. Quaternary surficial sediments derived directly from surrounding or buried sources will have a similar radiometric response to exposed source rocks, however transported detritus, containing mixed terrigenous material, will have a radiometric response consistent with its composite nature.

Radiometric data was used in conjunction with the magnetic data in order to attempt to map lithological variations. Images generated for this purpose included the radiometrics ternary image (Figure 3-5) and the radiometrics total count (Figure 3-6).

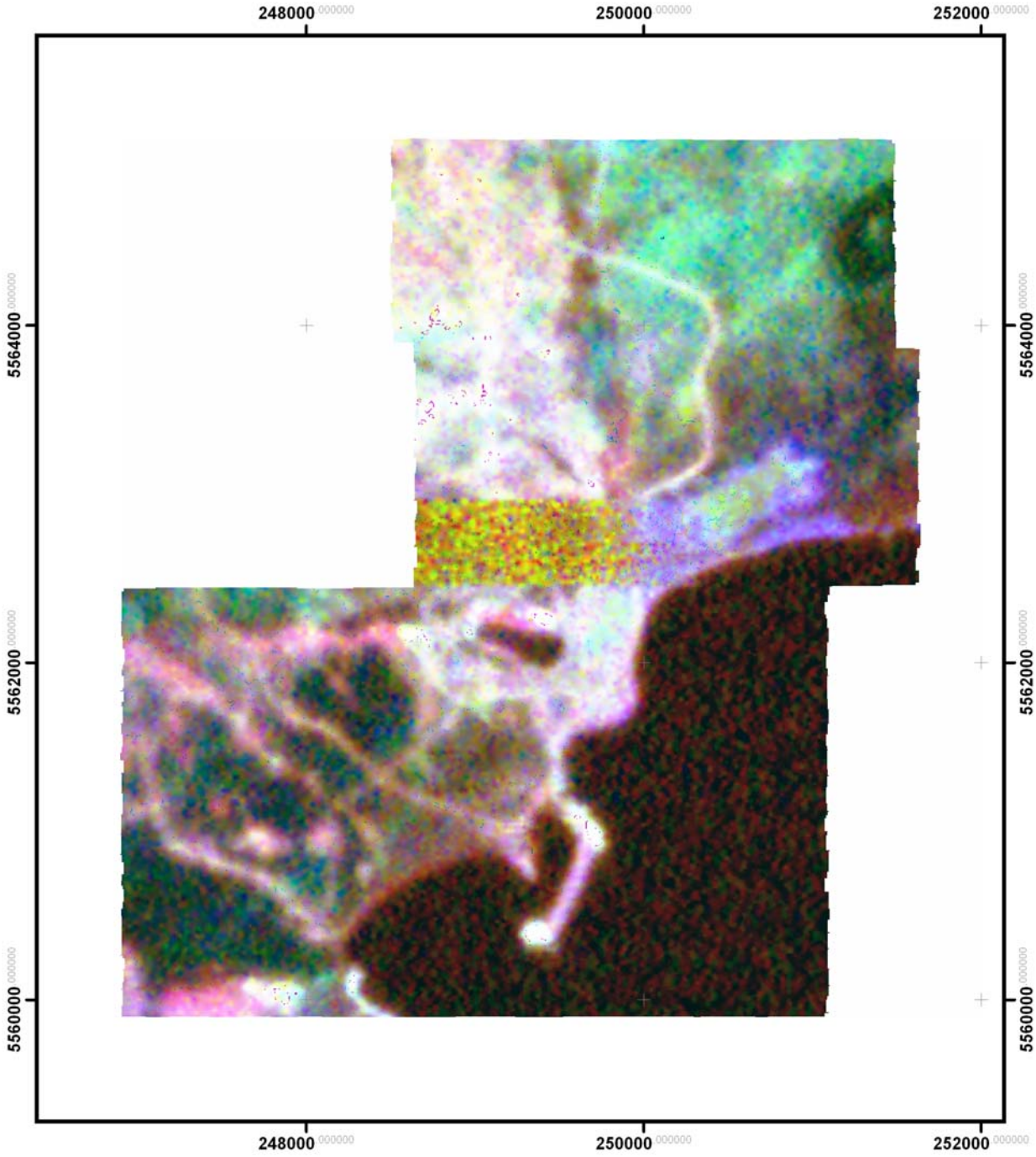

Figure 3-5: Radiometrics Ternary Image.

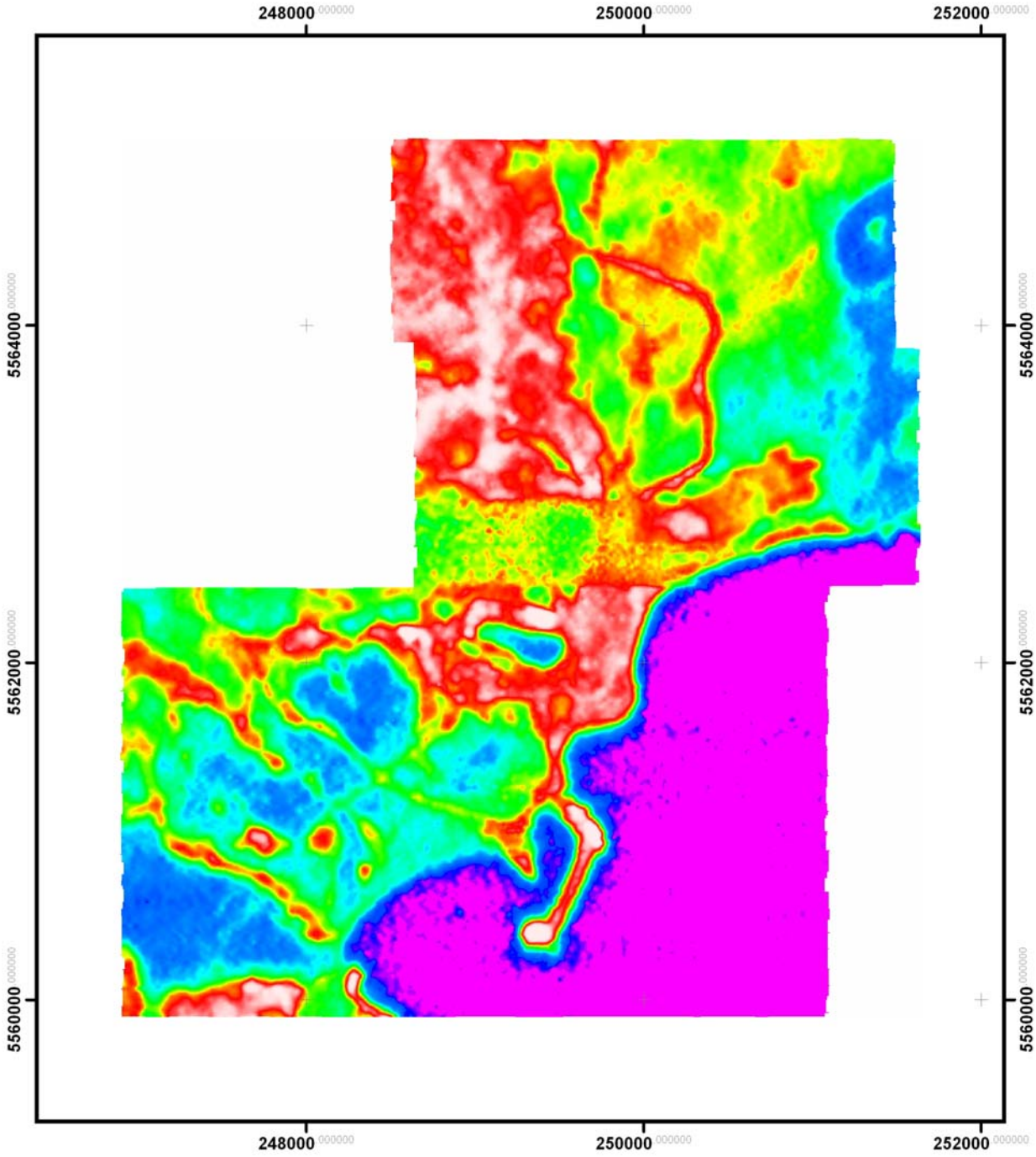

Figure 3-6: Radiometrics Total Count Image.

The **Ternary Image** is a combination of K (red), Th (green) and U (blue) data. Low response in all channels appears as black (e.g. over water), while high relative response in all channels appears as white. Coincident high counts in more than one channel combine to display as yellow hues (high Th & K), cyan hues (high Th & U) and magenta hues (high K & U). In regions of good outcrop or in arid climates where vegetation is less dominant, the various channels of

AGRS data can be used to accurately map changes in surface lithology. The Ternary image does not provide a quantitative representation of the radioactive elements, instead reflecting relative variations in radioactive element distribution.

Observations from the radiometrics **Total Count** and individual components can provide information that may not be visible in the combined Ternary image and may be useful for mapping alteration zones if K enrichment or significant quantities of U or Th mineralisation are present.

The E-W trending strip on the centre of the radiometric images is due to the helicopter having to increase survey altitude over the town of Grassy.

3.3 LANDSAT

In addition to the images of the magnetics and radiometrics data, images were produced from Landsat™ ETM7 data using different bands and ratios of bands. Landsat data images used include:

1. Bands 321 (Figure 3-7) and bands 741

2. Newton & Boyle: ratios of bands 7/5, 7/4, 5/1

3. CSIRO: ratios of bands 5/7 4/7 4/2

Landsat bands 1 through to 7 detect different features. These are listed in Table 1 below:

Table 1: Landsat bands and detection characteristics.

Band	Wavelength	Detects
1	Visual Blue	Water, iron-oxide features
2	Visual Green	Chlorophyll absorption and iron features
3	Visual Red	Chlorophyll absorption and iron features
4	Infrared	Iron absorption and vegetation
5	Short-wave infrared	Sulphates and water-bearing minerals (-OH absorption features)
6	Thermal infrared	Vegetation heat stress, soil moisture discrimination, and thermal mapping
7	Infrared	Hydroxyl-bearing minerals, clays, carbonates, mica, chlorite, and amphibole

The Landsat 321 image represents 'true' colour whereas the Landsat 741 image enhances linear structures, hydroxyl-bearing minerals, clays, carbonates, mica, chlorite, amphibole, water, and iron-oxide features. The Landsat CSIRO ratio discriminates between regolith units, phyllosilicates (including hydroxyl-bearing minerals) clays, carbonates, iron-oxides and vegetation. The Landsat Newton-Boyle ratios separate iron components from phyllosilicates including hydroxly-bearing minerals, clays, and carbonate as dark material.

Figure 3-7: Landsat 321 'True' Colour Image.

3.4 DIGITAL ELEVATION MODEL (DEM)

The Digital Elevation Model (Figure 3-8) is produced by subtracting the ground clearance of the aircraft (recorded by the radar altimeter), from the absolute height recorded by the GPS navigation system. This data is gridded in the same fashion as the magnetic data, and so has the same spatial resolution (5m cells). The DEM is used primarily to assist in mapping structurally related topographic features and to verify the significance and validity of radiometric data.

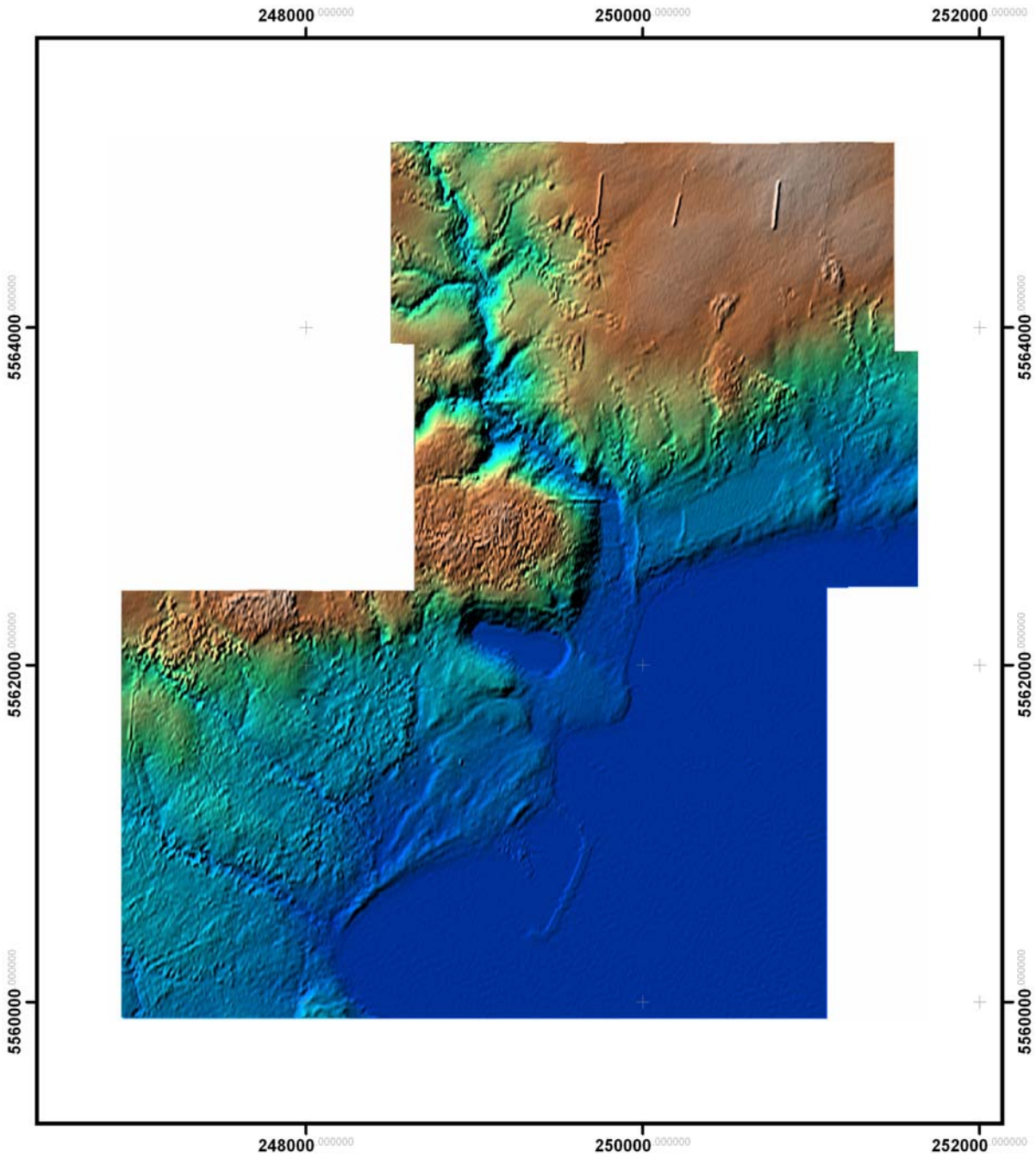

Figure 3-8: Digital Elevation Model.

4 INTERPRETATION

Magnetic and radiometric data have been used to create an integrated geological interpretation of the local area around Grassy covered by the airborne survey. A geological interpretation of the regional magnetic dataset was produced as a framework reference for the detailed Grassy interpretation. All the data necessary to undertake the integrated interpretation were geo-rectified and placed within a GIS. Data capture (points, lines, and polygons) for all interpretation work was done on-screen and recorded directly in digital format and the data (points, lines, polygons) are fully attributed.

4.1 REGIONAL INTERPRETATION

This interpretation was undertaken using the open file regional King Island magnetic dataset downloaded from the Geoscience Australia website (Table 2). These data were imaged and enhanced with RTP and 1VD filters (see section 3 for a description of these filters) for interpretation (Figure 4-1). The regional interpretation map and unit descriptions are presented in Figure 4-2 and Table 3.

Table 2: Regional survey data acquisition parameters

King Island Regional Airborne Survey Parameters	
Data aquired	Magnetics, radiometrics, elevation
Acquisition	Kevron Geophysics (Aeroplane)
Data of acquisition	2001
Line kms	8217
Line spacing (m)	200
Tie line spacing (m)	2000
Line orientation	090-270
Flying Height	80

The interpreted regional geology correlates well with the published mapped geology in terms of the spatial distribution of units (Figure 4-2 inset). It is beyond the scope of this project for a rigorous discussion of the regional interpretation to be presented. The following discussion highlights some observations of the interpretation which relate to the nature of the Devonian intrusions and the volcanics and sediments of the Grassy Group.

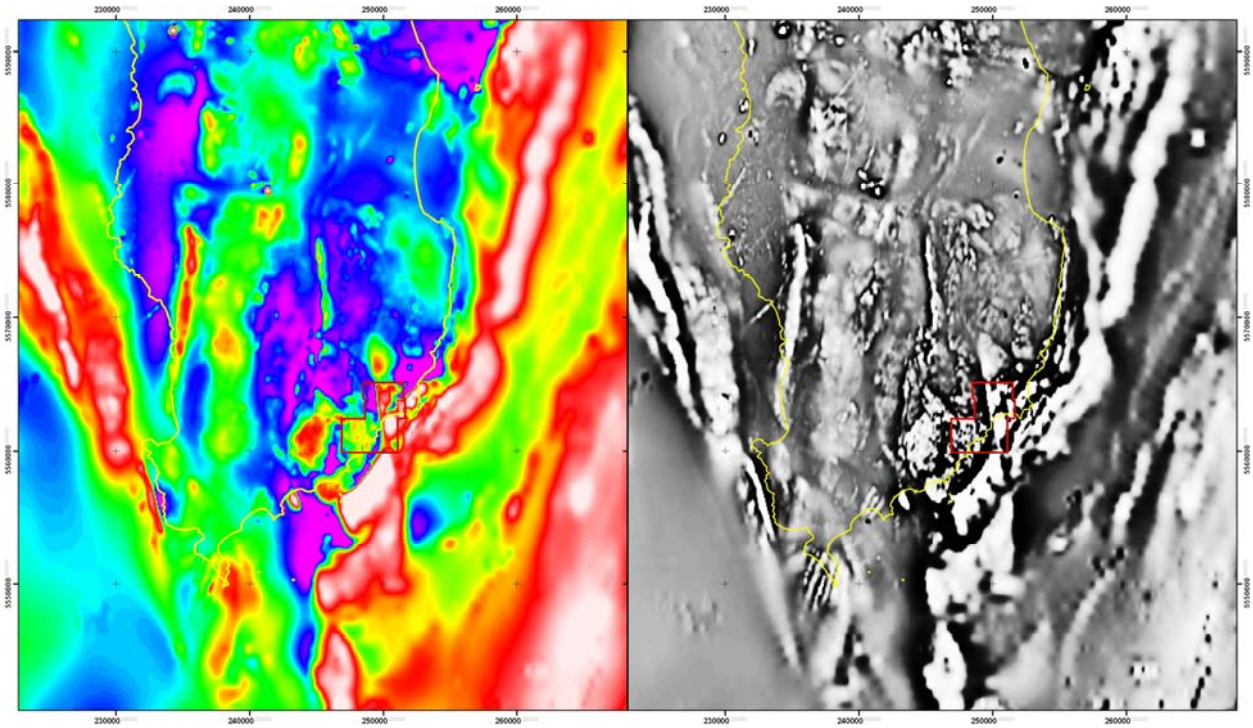

Figure 4-1: (a) Pseudocolour image of the TMI Reduced to Pole grid. (b) Greyscale image of the First Vertical Derivative of the TMI Reduced to Pole grid.

Grassy Group volcanosedimentary sequence

- The Grassy Group volcanosedimentary sequence is mapped offshore to the east and comprises a far greater extent of interlayered volcanics and sediments than mapped onshore (Figure 4-2). Strong linear northwest – southeast trending magnetic units offshore of the west coast are consistent with the presence of the Grassy Group volcanics.

- The sequence of Grassy Group volcanics to the west and east of the island dip southwest and southeast respectively. This suggests King Island represents a south plunging, north – south trending axial core of exhumed basement. The coincident north – south trending faults that crosscut the island, folding of the basement metasediments (particularly in the east), and emplacement of the Devonian Granite complex are all part of the Tabberabberan Orogeny (Gresham 1972) and associated with the axial exhumation of King Island.

Table 3: Lithological classification for regional interpretation based on the magnetic character on a 1VD RTP and TMI RTP magnetic images.

Age	*Stratigraphy*	*Unit*	*Frequency*	*Amplitude*	*Texture*	*Intensity*	*Lithology*
ca.400-360 Ma		Dg2	l	l	u-m	l	Devonian I-type Granite (Sea Elephant pluton)
		Dg1	h	h	m-s	l-m	Devonian I-type Granite (Grassy Pluton)
		Dg1a	h	m-l	m	h	Devonian I-type Granite (Bold Head Pluton also associated with the Grassy Pluton)
		Dm1	h	h	s-l	h-m	Devonian mafic bodies, large dykes, sills and plugs
c. 655--545 Ma	*Grassy Group*	Psv4	m-l	m	f-m	h-m	Mafic volcanics (covered by thick undifferentiated sediments)
		Psv3	m	m	l	h	Mafic volcanics
		Pss3	l	l	u-f	m	Undifferentiated sediments
		Pss2	l-m	l	u-l	m-l	Undifferentiated sediments
		Psv2	m-l	h	l	h	Mafic volcanics (possibly correlates with the Bold Head Volcanics)
		Psv1	h	h	l-m	h-m	Mafic volcanics (possibly correlates with the City of Melbourne and Shower Droplet volcanics)
		Pss1	h	h-m	m	m	Grassy Group
c. 760 Ma	*West Coast Granite*	Pg1	l	l	f-u	l	Batholithic S-type granite
c. 1000-750 Ma	*Naracoopa Formation*	Prm	h-m	h	l-s	m	Mafic bodies: large dykes, sills, plugs
		Prd2	h-m	l	m-u	l	Naracoopa Fm sediments above Devonian granite cupola.
		Prd1a	m	m	m-s	m	Naracoopa Fm sediments above high level Bold Head type granite marginal to main body.
		Prd1	h	m	l-m	l	Naracoopa Fm sediments above high level Devonian granite apophyses marginal to main body.
		Prp3	h-m	l-m	s-m	l	Metamorphic aurelal associated with Devonian granite emplacement
		Prp2	m	l	l-s	l	Basement (Surprise Bay Fm) sediments thinely covered by Naracoopa Fm sediments
		Prp1	l	l	f	l	Non magnetic sediments: shale, siltstone, fine-grained sandstone
c. 1300 Ma	*Surprise Bay Formation*	Ptd1	h-m	h	l-s	m-h	Surprise Fm. Metasediments above high-level Devonian granites
		Ptp3	h	h-m	l	m	Amphibolite, interlayered quartzofeldspathic schist and amphibolite
		Ptp2	m	l	s-u	m	Quartzofelspathic schist, includes pelitic to psammopelitic schist
		Ptp1	l	l	u	l-m	Psammitic to psammopelitic schist
		Pa	l	h	h	h-m	Mafic, magnetic metasedimentary schist
			h=high m=medium l=low	h=high m=medium	l=linear s=sublinear m=mottled u=undulose f=flat	h=high m=medium l=low	

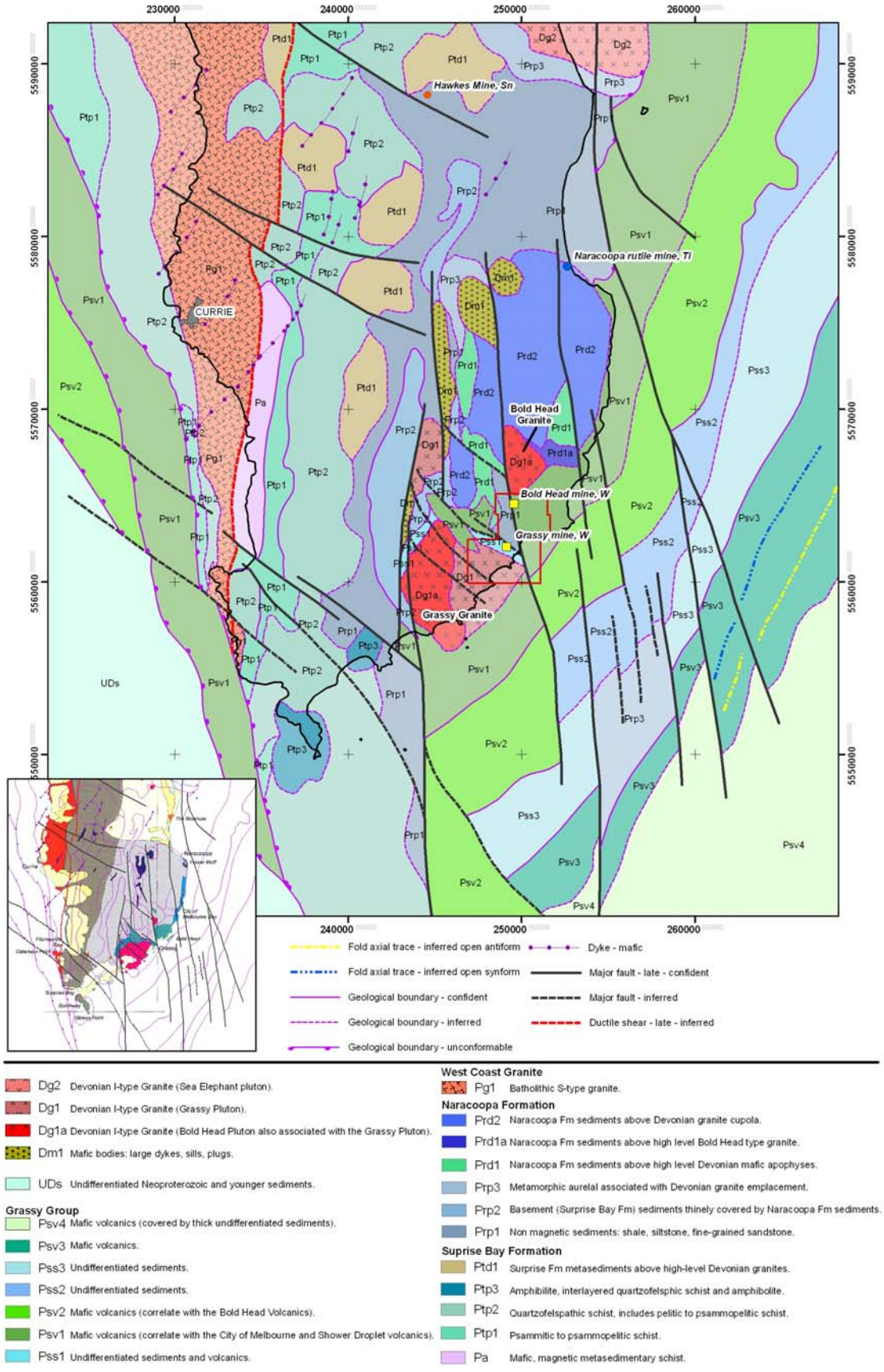

Figure 4-2: Geological interpretation map of the regional magnetic datasets undertaken by Fugro Airborne Surveys. Inset: published geology of King Island (see Figure 2-1) with overlayed interpreted linework (A3 inclusion at rear of report).

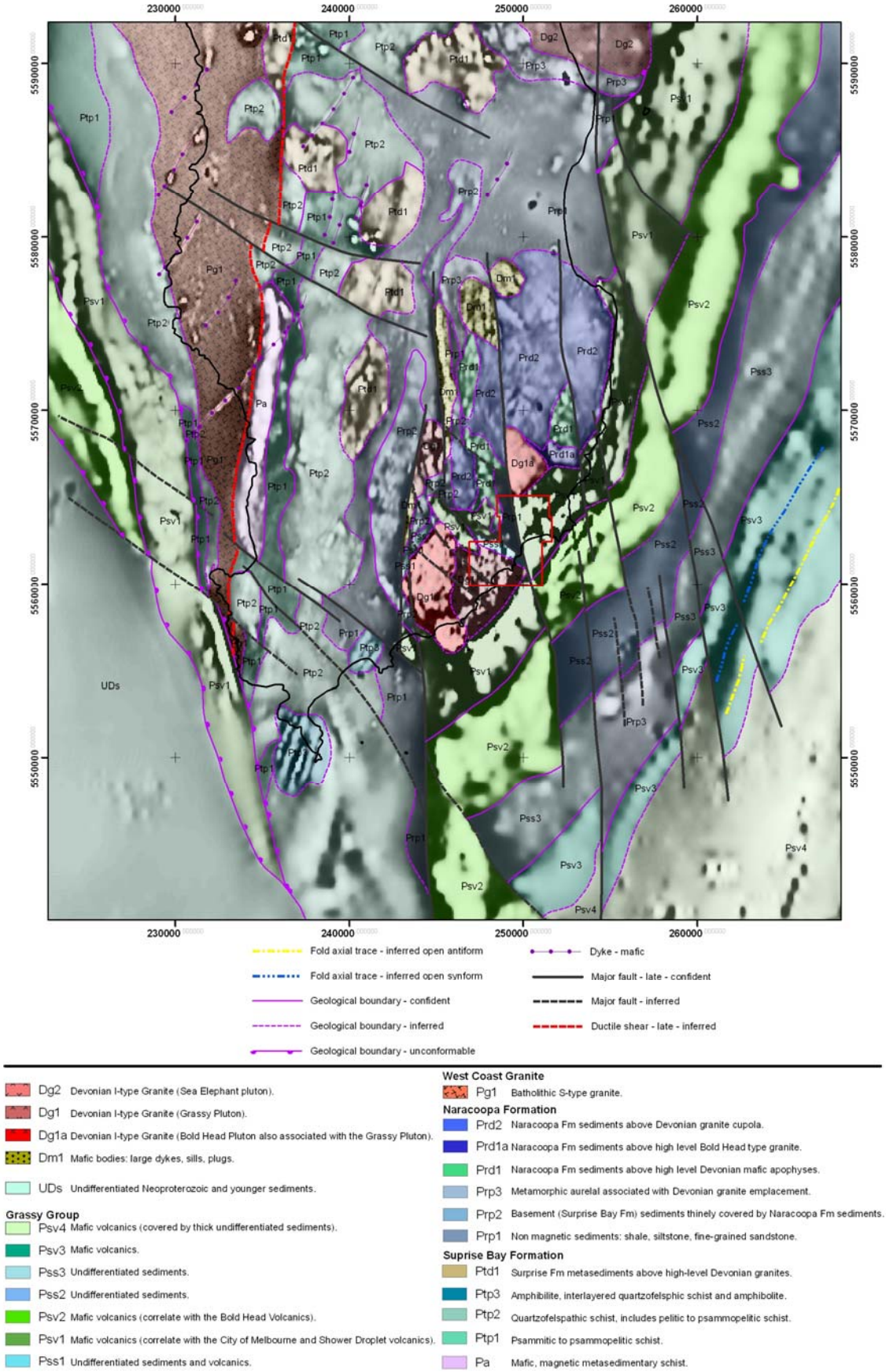

Figure 4-3: Geological interpretation map overlayed on the First Vertical Derivative of the TMI Reduced to Pole grid (A3 inclusion at rear of report).

Characteristics of the Devonian intrusions

- The Grassy Pluton is divided into two units based on distinct magnetic character (Figure 4-3). The Bold Head Pluton has the same magnetic character as the western unit of the Grassy Pluton and appears distinct from the unit associated with the Grassy Mine mineralisation.

- A greater extent of the Devonian granite complex is concealed beneath the Naracoopa Formation (unit Prd). These concealed intrusions are characterised by circular high- to moderate-frequency, subdued magnetic responses and maybe associated with smaller high-frequency bodies interpreted to represent high-level apophyses (Figure 4-3).

- Other potential concealed bodies of Devonian granite include a series of magnetic units (unit Ptd1) along the margin between the Naracoopa and Surprise formations (Figure 4-2).

- A prominent set of north – south trending faults occur across the central and eastern area of the island. These structures are associated with an apparent sinistral offset of the majority of mapped units. Only some of the late phases of the Devonian granite complex appear to have a synchronous timing relationship with these faults. A second set of northwest – southeast trending faults ramp out from and link between the north – south trending faults. Calver (2007) considers the Bold Head Pluton to have been sinistrally offset from the Grassy Pluton by the Grassy River Fault. However Gresham (1972) ruled out this possibility based on the distinctive magnetic characteristics between the two bodies and suggests that displacement was primarily dip slip along the Grassy River Fault.

  These northwest – southeast trending subsidiary structures are inferred to represent extensional structures (which include the Swan and Central faults in the Grassy mine area) and link with the main north – south trending structures which may have extensional to a sinistral transtensional component of displacement.

- The mapped mafic bodies considered to represent lopolithic type intrusions (Gresham 1972) correlate with distinct high frequency magnetic responses (Figure 4-3). The bodies are marginal to the interpreted greater Devonian granite intrusions and as elongate bodies along the late north – south trending faults. The close spatial association and the cross-cutting contact relationship with the granites are consistent with these mafic bodies representing late emplaced phases of the Devonian granite complex.

- The emplacement of the mafic bodies along the north – south trending faults indicates a late synchronous timing of faulting with intrusion of the Devonian granite complex. This timing is consistent with the observed fault controls on the scheelite mineralisation at the Grassy Mine (Calver 2007). These observations have significant implications for understanding the controls on the mineralisation.

Observations from this regional study show these north – south structures crosscut the main granite bodies (including the extensive concealed bodies) and are considered to have been contemporaneous with the emplacement of the late stage mafic bodies. **Therefore the mineralisation associated with the Grassy Mine may not only be related to the emplacement of the Grassy Pluton. A secondary control maybe the faulting along which late stage enriched fluids were focussed into the pre-prepared contact aureole of the Grassy Pluton. Hornfels development within the Grassy Group sediments around the Grassy Pluton probably played an important role in pre-preparing the ground for brittle faulting and preferential dilation for secondary fluid ingress.** This is consistent with the observed overprinting mineralisation, the association of scheelite in joints and veins and the association of late stage sulphide mineralisation near the major faults (Calver 2007). **These secondary high-grading conditions maybe an important requirement for the development of economic reserves and therefore is an important exploration criterion to consider.**

4.2 INTEGRATED SOLID GEOLOGY INTERPRETATION

Magnetic, radiometric, DEM and Landsat images have been used to create an integrated geological interpretation of the area around the King Island Scheelite Mine. Comparing this interpretation with available geological maps of the survey area has allowed the classification of the local lithological units with respect to the geophysical data. The classification scheme, based on the magnetic response from each unit, is presented in Table 4 with the resulting final map product is shown in Figure 4-4.

Important features in the survey area include:

- The Grassy River Fault has had a complex reactivation history. The initial displacement probably accommodated largest component of movement. This was crosscut by a regional southwest - northeast trending fault that resulted in approximately 1km of apparent sinistral offset (Figure 4-4) Subsequent reactivation along the Grassy River Fault truncated the southwest - northeast trending fault zone and propagating south

around the margin of the Grassy Granite. This latter structure is the Decline Fault (Figure 4-4).

- The possible presence of mine series rocks (Pss1) between the Decline Fault and the displaced Grassy River Fault.

- The response from the Grassy Granite along its eastern boundary (a change in magnetic amplitude and texture) indicates either two phases of intrusion or a shelving of the granite contact at depth.

- A distinct change in the magnetic properties of the extensive volcanic sequence east of the Grassy River Fault, defines a series of separate volcanic units.

- This volcanic sequence comprises complex, northwest – southeast trending minor fault sets related to the Grassy River Fault. These fault sets are consistent with similar oriented structures mapped within the mine area and more extensively in the regional interpretation.

Table 4: Lithological classification based on magnetic response.

Lithological Classification	Magnetic Amplitude	Magnetic Frequency	Magnetic Texture
Lower Neoproterozoic siltstone (quartzites and siltstones)			
Prp1	l	l	flat
Prp1a	m	m	sublinear
Upper Neoproterozoic diamictite, dolostone and shale (Mine Series)			
Pss1	l	l	flat
Upper Neoproterozoic basaltic volcanic rocks (Volcanics)			
Psv1	v	m	mottled
Psv1a	m	m	sublinear
Psv1b	h	m	sublinear
Psv1c	l	m	sublinear
Upper Neoproterozoic undifferentiated sediments			
Pss1a	m	m	sublinear
Devonian (Grassy) Granite			
Dg1	h	m	mottled
Dg1b	m	m	mottled

(l = low, m = moderate, h = high, v = very high)

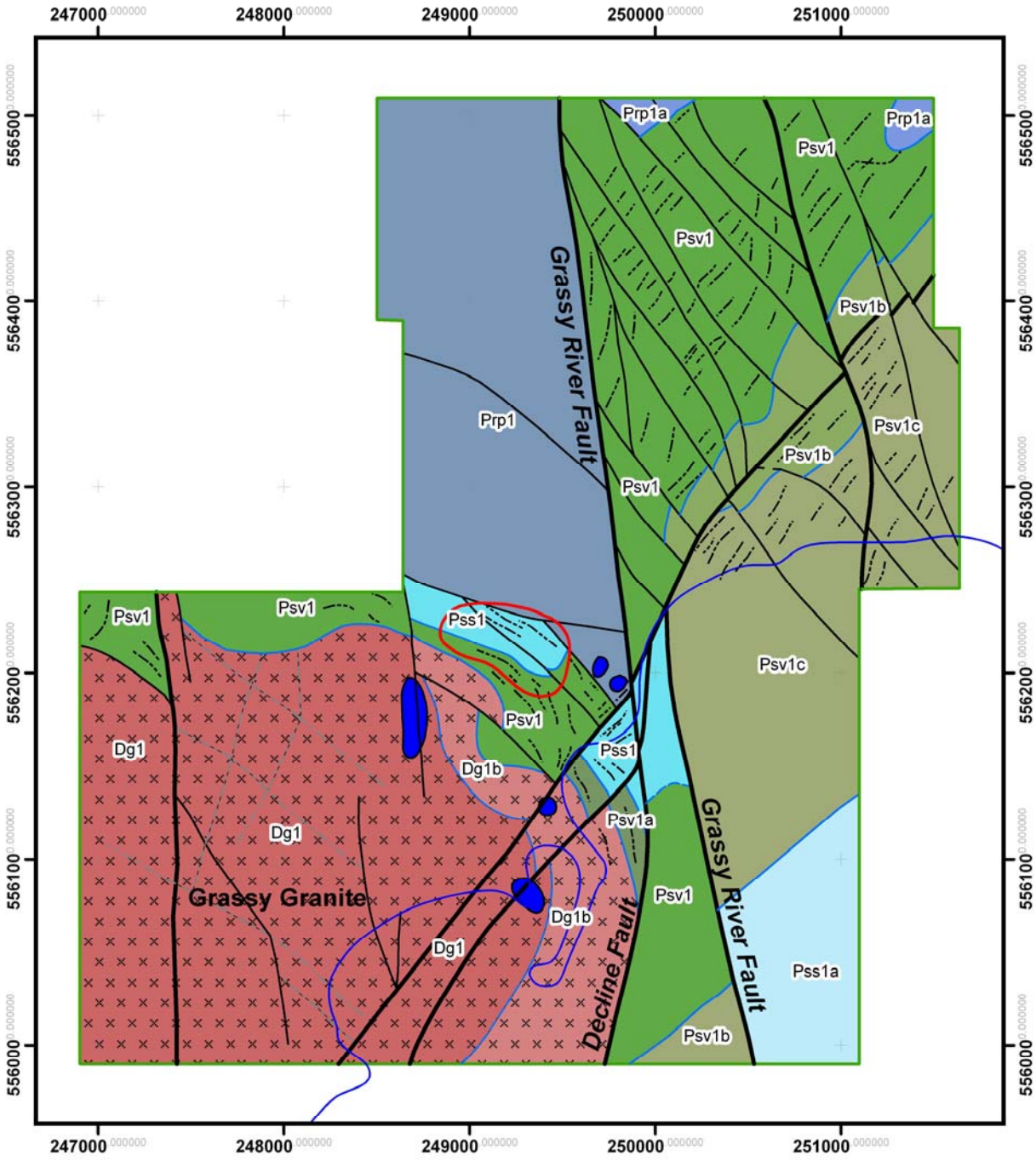

Figure 4-4: Integrated geological interpretation (see over for legend).

LEGEND

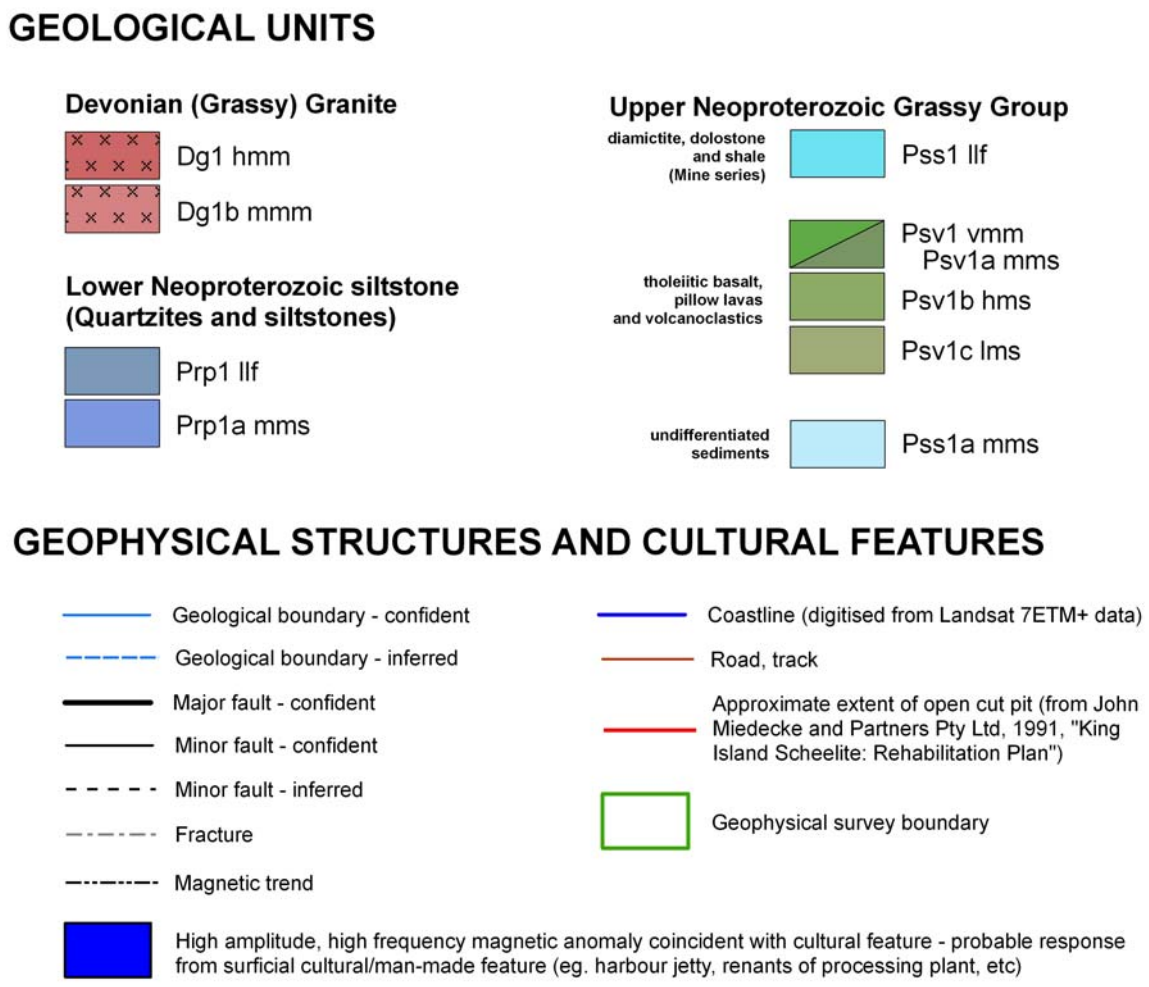

The interpretation would suggest that the area around Grassy has been subject to a complex deformation history. This is best exemplified by the Grassy River Fault which, from the regional dataset, appears to have offset the Bold Head Granite from the Grassy Granite. The geological interpretation indicates that subsequent to this, the fault was offset before being reactivated, resulting in the formation of the Decline Fault. During this time the numerous subsidiary structures visible in the volcanics to the east were also formed.

It is postulated that there is an extension of the Grassy orebody to the southeast, beneath Grassy Bay (King Island Scheelite Limited 2006). **The existence and extent of this possible orebody, named the 'Toredo' extension, cannot be confirmed from the interpretation of the geophysical data. However interpretation supports the presence of Mine Series rocks to the east of Decline Fault, possibly to the contact with the Grassy River Fault, and also to the southeast of the open cut pit, beneath Grassy Bay. Such mine series rocks could provide a suitable host unit for an extension to the orebody.**

The Grassy orebody does not exhibit a magnetic signature which can be resolved within these Mine Series rocks. Considering the moderate magnetic susceptibility values of the skarn (0.006SI, value supplied by King Island Scheelite Limited) and the thickness of the B and C Lens horizons this is not surprising. **Therefore a localised magnetic signature within these mine series rocks would not be anticipated to provide any direct indication for the 'Toredo' extension**. In comparison, although the Grassy Granite has a lower magnetic susceptibility of 0.004SI it has a larger magnetic susceptibility/thickness product due to the larger volume of rock. Hence it shows a higher amplitude Total Magnetic Intensity response.

5 QUANTITATIVE MAGNETIC INTERPRETATION

One of the objectives of the project was to undertake a quantitative source depth study of the magnetic data to provide an estimate of the thickness waste materials and beach deposits overlying deeper 'magnetic basement' in the area immediately adjacent to the 'sea dump'. By extending this study to include all areas within the survey boundaries underlying the sea it has been possible to provide an indication of the depth to 'magnetic basement'. Additionally, profile modelling was undertaken in order estimate the dip of the major north-north-west trending fault structure.

To meet these aims quantitative interpretation was carried out utilising two different methodologies:

- Automated interpretation of both profile data. This has involved 2D Werner deconvolution of profile data to estimate depth to basement.
- Profile modelling and inversion. The magnetic results are integrated with the qualitative interpretation and all other available datasets to provide an overall interpretation framework.

5.1 WERNER DECONVOLUTION

Werner deconvolution modelling was carried out to determine the depth to the magnetic basement rocks in the offshore portion of the survey area, with a particular emphasis in the old sea dump and over the northern area where the main N-S fault runs. The following parameters were used in the Werner analysis:

Grid cell size	5m & 15m
Min window length	60m
Max window length	500m
Min depth	30m
Max depth	250m
Window expansion increment	20m
Window shift increment	20m
Field strength (average)	61219nT
Inclination	-70.8^{O}
Declination	12.1^{O}

Filtering was applied to the magnetic data to remove the highest frequency components before Werner deconvolution was undertaken. In order to exclude the Werner solutions that were deemed to be outliers, two cluster analyses were run over the depth solutions database. The

first clusters were determined with a vertical window size of 10m by 10m along the flight lines. A second cluster analysis was run over the results of the first where the lateral and vertical extent of the window was doubled to 20m x 20m (4 x area) (Figure 5-1). These operations had the effect of lowering the standard deviation substantially of the final data points used for gridding. Additionally, spurious depth solutions caused by magnetic anomalies resulting from cultural features were screened manually. The final grids were filtered using a Hanning filter to further reduce the high frequency effects of any remaining outliers.

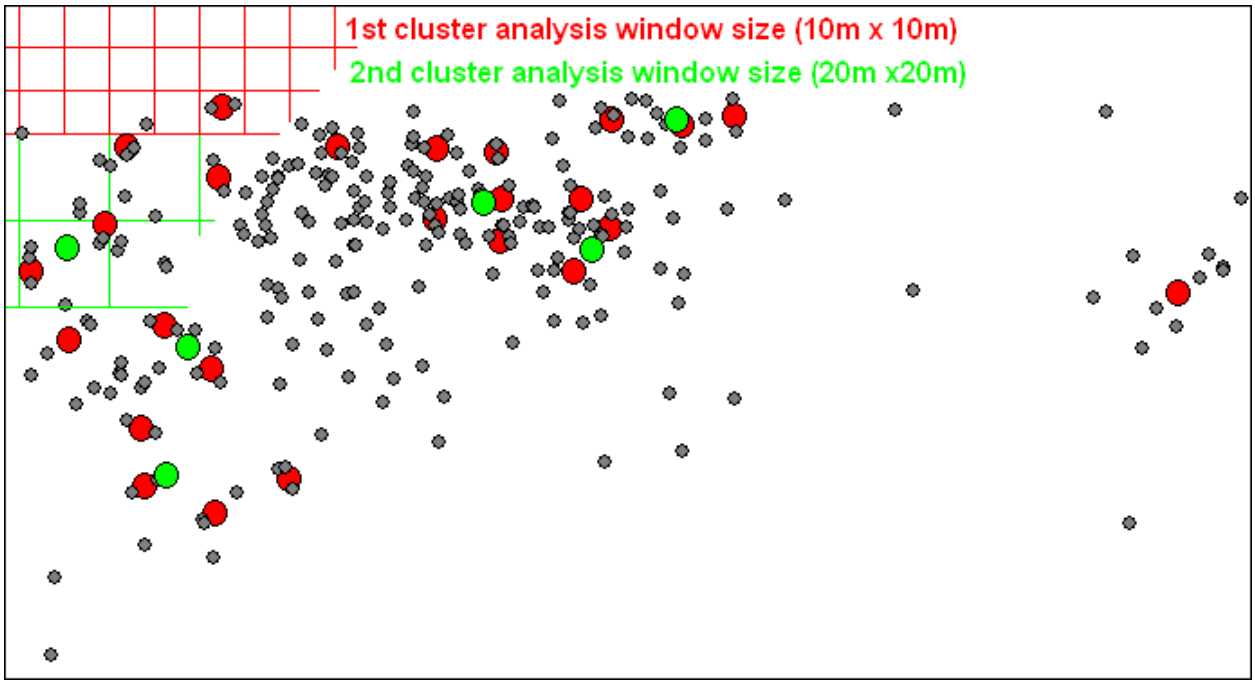

Figure 5-1: Cluster analyses to exclude outlier depth solutions (grey dots). Red dots show the results of the first pass and the green dots are the results of the second pass (example not to scale).

The results of the Werner deconvolution modelling are presented as a map of Depth to Magnetic Basement (Figure 5-2).

The map shows that there is a general increase in depth to magnetic basement across the eastern half of the grid, with a marked increase along an approximate north - south trend located just to the east of the sea dump and harbour wall. Comparison with the interpreted solid geology map indicates the change in depth to be coincident with the location of the major north - south trending Decline Fault identified in the magnetic data.

To the east of the Decline Fault the depth to magnetic basement increases significantly, in some areas to over 150m below datum. This area extends to the east to the interpreted location

of the Grassy River Fault. East of the Grassy River Fault the depths are variable, ranging from 10 to 100m below datum, indicating an undulating upper surface of the magnetic basement.

Elsewhere, results compare well with the limited drill log data available. It is known from two boreholes drilled through the old sea dump material that the thickness of non-magnetic, unconsolidated deposits increases quite rapidly, from approximately 30m to over 60m (Robin Morritt, personal communication). The depth to basement model correlates well with this information showing a general increase in depth from west to east. It is unclear whether the increase is the result of thickening unconsolidated sediments or a fault structure with vertical offset, though a fault has been identified running through the area.

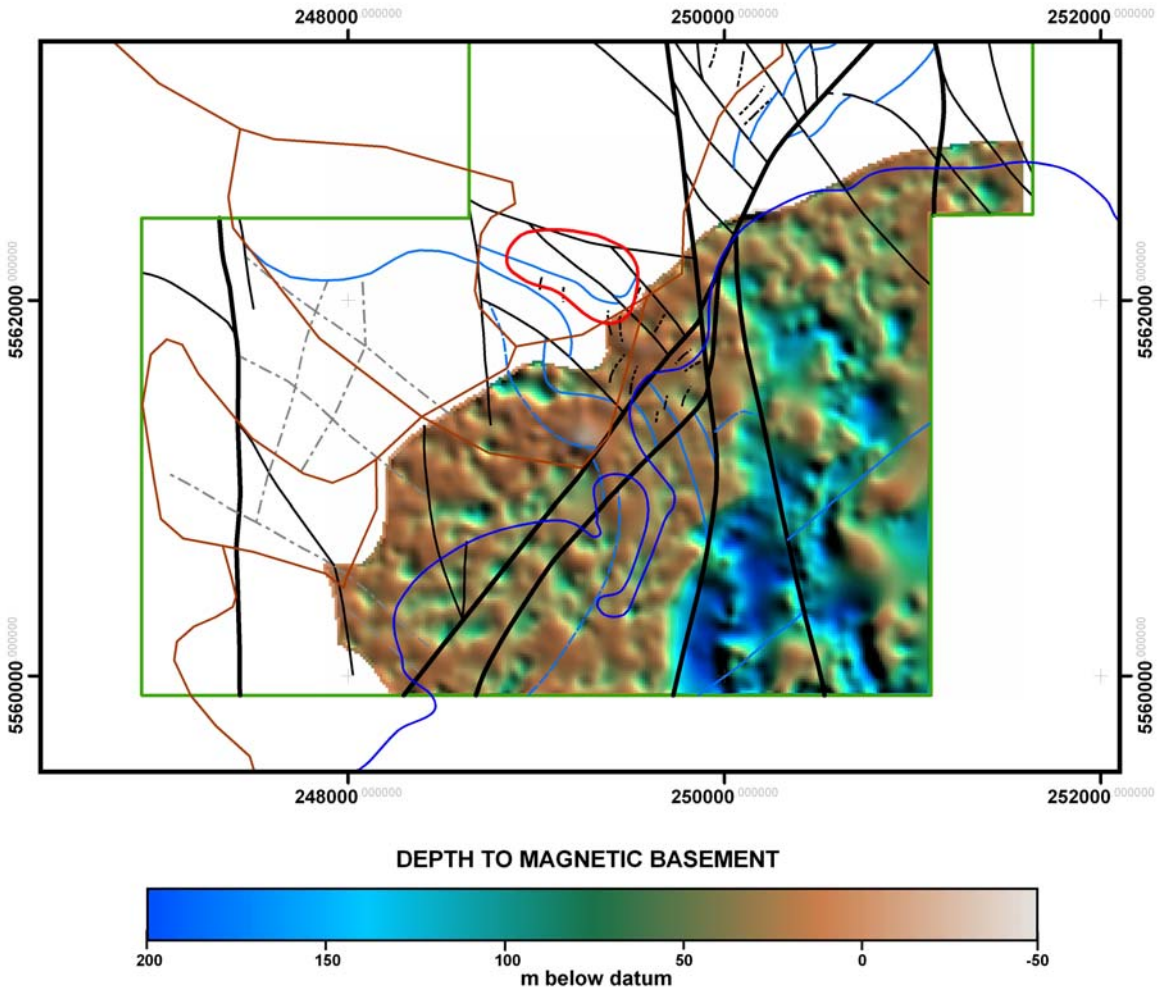

Figure 5-2: Depth below sea level of the magnetic basement calculated from Werner deconvolution modelling. The blue line shows the coastline (digitised from aerial photos) and the green line shows the extents of the airborne survey (A3 inclusion at rear of report).

It should be noted that the depth to magnetic basement may not equate to the depth to consolidated material. Consolidated, non-magnetic sediments may overly the 'magnetic basement' being modelled.

5.2 PROFILE MODELLING

Modelling of the magnetic anomaly resulting from the Grassy River Fault to the north of Grassy was carried out along a number of flightlines using ModelVision Pro software from Encom. The main aim of the modelling process was to determine the dip of the Grassy River Fault.

Simple block models with magnetic susceptibility values ranging from 0.009 to 0.034SI were generated to represent the volcanic sequence located to the east of the Grassy River Fault. The extremely low susceptibility values for the quartzites (<0.0005SI) excluded the requirement for block models to be generated for the sequences west of the fault. Magnetic susceptibility values were based on measured data provided by King Island Scheelite Limited.

Although the uppermost magnetic susceptibility values used for the volcanics appear quite large in comparison with the average measured value of 0.013SI, they are not considered unrealistic. The measured data shows a standard deviation of 0.020SI and a maximum recorded value of 0.093SI.

Representative examples of the results of the modelling along lines L10044 (5564235N) and L10064 (5563840N) are presented in Figure 5-3 and Figure 5-4. In these examples the upper pane shows the measured data (black line), modelled data (red line) and calculated regional field (blue line). The left hand axis shows values in nanoTeslas whilst the horizontal axis represents distance along the line. The lower pane shows the generated model along with the calculated DTM (red line) and the altitude of the aircraft (blue line). The left hand axis shows the depth below datum in metres whilst the horizontal axis represents distance along the line.

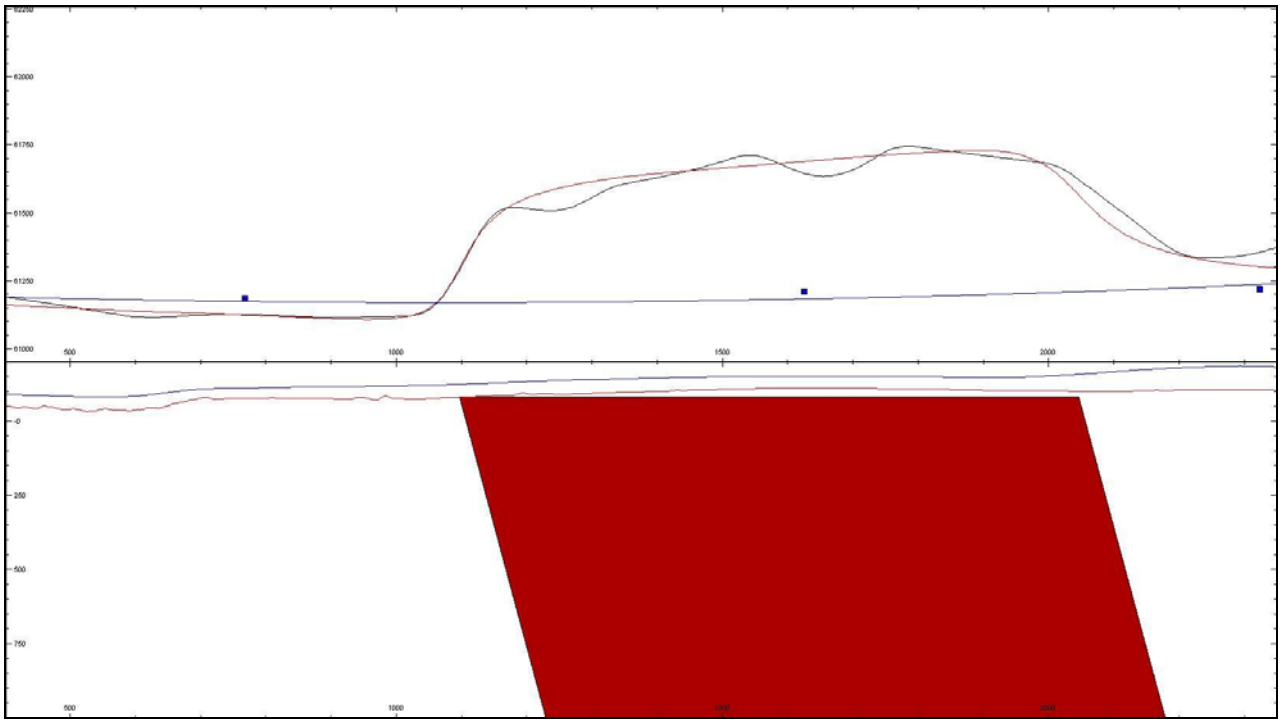

Figure 5-3: Simple profile model along line L10044 (5564235N).

The modelled profile along line L10044 shows a good fit with the recorded data despite the simplified model used. A single body was used to represent the volcanic rocks. By interactively adjusting the properties of the body a very good fit was obtained between the measured and modelled data at the location of the fault (approximately 1100m along line) with a reasonable fit elsewhere. **Results provided a sub-vertical dip of 83^{o} to the east for the Grassy River Fault.**

In order to model the undulations observed in the magnetic data to the east of the fault along line L10064 six separate block models, each with individual magnetic susceptibilities, were used. As with the previous line the properties of the bodies were interactively adjusted to obtain a good fit between the measured and modelled data. Results for this model were consistent with the previous results, modelled dip being 85^{o} to the east.

The presence of younger, volcanosedimentary rocks to the east of the fault in comparison to the Lower Neoproterozoic quartzites and siltstones to the west provide an indication that this structure is a normal fault.

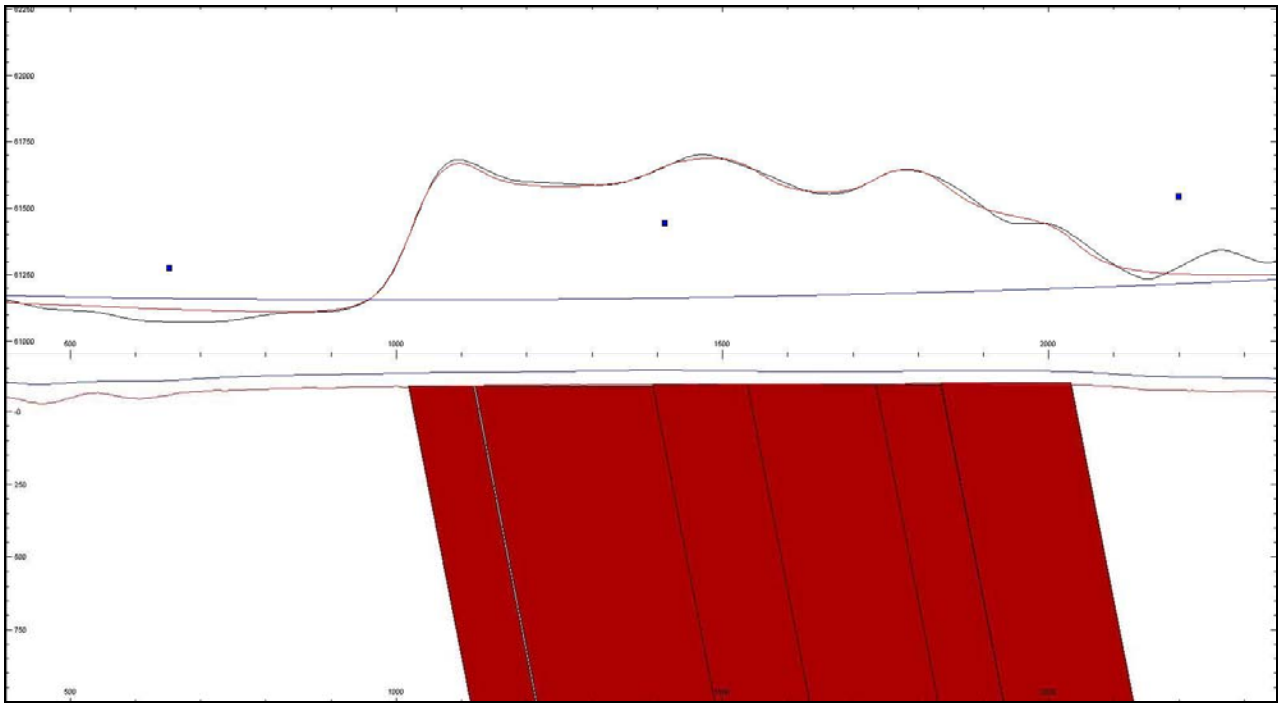

Figure 5-4: Simple profile model along line L10064 (5563840N).

6 RESULTS AND CONCLUSIONS

Fugro Airborne Surveys - Perth (FASP) was contracted by King Island Scheelite Limited to interpret airborne magnetic and radiometric data from Grassy, King Island. The objective of the geophysical interpretation was multi-fold. A geological interpretation of the solid geology of both the airborne survey and open source data were undertaken. Cultural data, such as roads, towns, place names and areas of previous investigation were incorporated into these datasets.

Interpretation of the regional datasets correlates well with the published mapped geology in terms of the spatial distribution of units (Figure 4-2 inset). Of interest for this particular project, in terms of understanding the controls on the mineralisation, is the interpretation of the timing of the north – south fault structures.

The evident control on the emplacement of late phase mafic bodies suggests the timing of the regional north – south faults to be late synchronous with the intrusion of the Devonian granites. As a result the scheelite mineralisation may not be solely related to the Grassy Granite pluton, localised faulting may have acted as a secondary control to allow enriched late stage fluids into the metamorphic aureole.

Similarly, interpretation of the high resolution airborne geophysical data has made it possible to produce an integrated geological map of the survey area with lithologies identified by comparison with other available geological maps of the area (Calver 2007; Brown 1981; Brown 1975; Gresham 1972). Comparison of these historical references with the integrated geological map shows a strong correlation between all datasets.

The interpretation has identified numerous fault structures within the survey area, many located in close proximity to the open cut pit. In light of the proposed extension of the pit to the south east into Grassy Bay these faults may present engineering problems, presenting pathways for the influx of seawater.

It has been postulated that there is an extension of the Grassy orebody to the southeast, beneath Grassy Bay (King Island Scheelite Limited 2006). There is no direct magnetic evidence to support the postulated 'Toredo' extension to the southeast of the main orebody. However it is not considered likely that the ore bodies will be magnetic due to the low magnetic response of the skarn and the size of the B and C lens horizons. The geological interpretation does however support the presence of Mine Series rocks both to the east of Decline Fault, possibly to the contact with the Grassy River Fault, and to

the southeast of the open cut pit, beneath Grassy Bay, providing suitable host units for such an ore body.

Werner deconvolution modelling of the magnetic data has produced a 'depth to magnetic basement' map. **Sharp changes in the topography of this basement surface appear coincident with mapped fault structures whilst across the old sea dump area there is a localised increase in the thickness of non-magnetic, unconsolidated deposits**. This information correlates well with data from two boreholes located in the area which drilled through overburden with a thickness of 30m to the west of the dump and 60m to the east before reaching solid basement material. It is unclear whether the increase is the result of thickening unconsolidated sediments or a fault structure with vertical offset, though a fault has been identified running through the area.

It should be noted that the depth to magnetic basement may not equate to the depth to consolidated material. Consolidated, non-magnetic sediments may overly the 'magnetic basement' being modelled.

Profile modelling across the Grassy River Fault identified this structure to be sub-vertical, dipping at approximately 85^{o} to the east. The presence of younger, volcanosedimentary rocks to the east of the fault in comparison to the Lower Neoproterozoic quartzites and siltstones to the west provide an indication that this structure had a normal component of displacement.

7 REFERENCES

Baranov, V. 1957, 'A new method for interpretation of aeromagnetic maps – pseudo gravimetric anomalies', *Geophysics,* vol. 22, pp. 359-383.

Berry, R.F., Holm, O.H. & Steele, D.A., 2005 'Chemical U-Th-Pb dating and the Proterozoic history of King Island, southeast Australia', *Australian Journal of Earth Sciences,* vol. 52, pp. 461 – 471

Black, L.P., Seymour, D.B., Corbett, K.D., Cox, S.E., Streit, J.E., Bottrill, R.S., Calver, C.R., Everard, J.L., Green, G.R., McClenaghan, M.P., Pemberton, J., Taheri, J. & Turner N.J., 1995 'Dating Tasmania's oldest events' *Record Australian Geological Survey Organisation 1997/15*

Black, L.P., Calver, C.R., Seymour, D.B. & Reed, A., 2004 'SHRIMP U-Pb detrital zircon ages from Proterozoic and early Palaeozoic sandstones, and their bearing on the early geological evolution of Tasmania' *Australian Journal of Earth Sciences,* vol. 51, pp. 885 - 900

Brown, S.G., 1981, 'Progress Report on Exploration Licence 15/66 for the Six Months Ended 24th October 1981' *Geopeko Limited Report No. KI/81/4*

Brown, S.G., 1975, 'Progress Report on the Exploration of the Grassy Granite Contact Zone' *Geopeko Limited Report No. KI/75/3*

Calver, C.R. & Walter, M.R. 2000 'The late Neoproterozoic Grassy Group of King Island, Tasmania: correlation and palaeogeographic significance' *Precambrian Research,* vol. 100, pp 299 - 312

Calver, C.R. 2007 'Some notes on the geology of King Island', *Tasmanian Geological Survey Record 2007/02*

Cox, S.F. 1989 'Cape Wickham', in Burrett, C.F. and Martin, C.F. (ed) 'Geology and Mineral Resources of Tasmania', *Special Publication Geological Society of Australia,* vol. 15, pp 26 - 27

Crawford, A.J., Stevens, B.P.J., Fanning, M. 1997 'Geochemistry and tectonic setting of some Neoproterozoic and Early Cambrian volcanics in western New South Wales' *Australian Journal of Earth Sciences,* vol. 44, pp. 831 – 852

Direen, N.G. & Crawford, A.J. 2003 'The Tasman line: Where is it, what is it, and is it Australia's Rodinian breakup boundary?' *Australian Journal of Earth Sciences,* vol. 50, pp. 491 – 502

Gresham, J.J. 1972. 'The Regional Geology of King Island', *Geopeko Limited Report*

Gunn, P.J., Fitzgerald, D, Yassi, N. & Dart, P. 1997, 'New algorithms for visually enhancing airborne geophysical data', *Exploration Geophysics,* vol. 28, pp. 220-224.

King Island Scheelite Limited, 2006 'King Island Scheelite Mine Redevelopment Feasibility Study – Executive Summary'

Knight, C.L. & Nye, P.B. (Revised by staff of King Island Scheelite Ltd), 1957 'Scheelite Deposit of King Island', in *The Geology of Australian Ore Deposits* 2nd. Ed (Ed. J. McAndrew), pp515 - 517

Ku, C. C., and J. A. Sharp, Werner deconvolution for automated magnetic interpretation and its refinement using Marquart's inverse modelling, Geophysics,48(6),754-774, 1983

Leaman, D.E., 2003 'The form of the King Island and Beulah granites' *Tasmanian Geological Survey Record 2003/06*

Meffre, S. Direen, N.G., Crawford, A.J. & Kamenetsky, V. 2004 'Mafic volcanic rocks on King Island, Tasmania: evidence for 579Ma break-up in east Gondwana' *Precambrian Research,* vol. 135, pp 177 - 191

Nabighian, M.N. 1972, 'The analytic signal of two-dimensional bodies with polygonal cross-section: its properties and use for automated interpretation', *Geophysics*, vol. 37, pp. 507-517.

Phillips, J. D., Potential-Field Geophysical Software for the PC, version 2.2: USGS open-File Report 97-725, 1997

Telford, W. M., L. P. Geldart and R. E. Sheriff, Applied Geophysics, 1990

Turner, N.J., Black, L.P. & Kamperman, M. 1998 'Dating of Neoproterozoic and Cambrian orogenies in Tasmania', *Australian Journal of Earth Sciences,* vol. 45, pp. 789 - 806

Werner, S. 1953, 'Interpretation of magnetic anomalies of sheet-like bodies', *S.G.U. ARSBOK*, vol. 43.

8 APPENDIX 1 – QUANTITATIVE MAGNETIC INTERPRETATION METHODS

8.1 WERNER DECONVOLUTION

Werner deconvolution is a semi-automated depth-to-magnetic source technique designed for the interpretation of magnetic profile data. The method was originally proposed by Werner (1953) and derives estimations of depth to either a dyke (or thin body) or geological contact.

In principle it is possible to estimate the location of the top of a body and its magnetisation from only four measurements of the TMI anomaly. By dividing a profile of TMI measurements into groups of four or more readings, an estimate of the source location can be estimated for each group. Plotting these estimates in cross section results in a cluster of solutions around the true location of the sheet-like body.

Werner's equation is derived from the analytical expression for a thin sheet of diploes:

$$F(x) = \frac{A(x - x_0) + Bz}{(x - x_0)^2 + z^2} \quad (8.1.1)$$

where x_0 is the surface point directly above the centre of the top of the dyke, z is the depth to the top, x is the point of measurement and the *x* axis is normal to strike. A and B are unknown functions of the dyke geometry and mineralisation (Telford et al. 1990). This equation can be rearranged to the form:

$$x^2 F(x) = a_0 + a_1 x + b_0 F(x) + b_1 x F(x) \quad (8.1.2)$$

where $a_0 = -Ax_0 + Bz$, $a_1 = A$, $b_0 = -x_0^2 - z^2$ and $b_1 = 2x_0$, giving $x_0 = b_1/2$ and $z = \sqrt{(-4b_0 - b_1^2)}/2$. x_0 and z can be determined by measuring F at four stations, generating a system of Werner equations which can be inverted solving equation (8.1.2) for a_0, a_1, b_0 and b_1. These expressions provide the location of the top of the dyke as well as the magnetic susceptibility and dip parameters.

To represent the effects of interference from neighbouring anomalies and the regional field, a polynomial curve can be used in the equation, such that the measured field $\mathcal{F}$ is given by:.

$$\mathcal{F} = F(x) + c_0 + c_1 x + ... + c_n x^n \quad (8.1.3)$$

where $F(x)$ is given by equation (8.1.1) so that there are $(n+5)$ unknown quantities involved.

In order to solve these unknown parameters, a window of data with at least 7 points is taken from the profile and the parameters are found using inversion. The window is moved along the profile potentially generating a solution for each window location. Additionally, as deeper magnetic sources typically generate longer wavelength anomalies to sample longer wavelength anomalies it is necessary to use a larger window size. Increasing the window size by extracting every nth point from the profile, where n is known as the lag (Figure 8-1), allows analysis of longer wavelength anomalies while maintaining the same number of sampled data points.

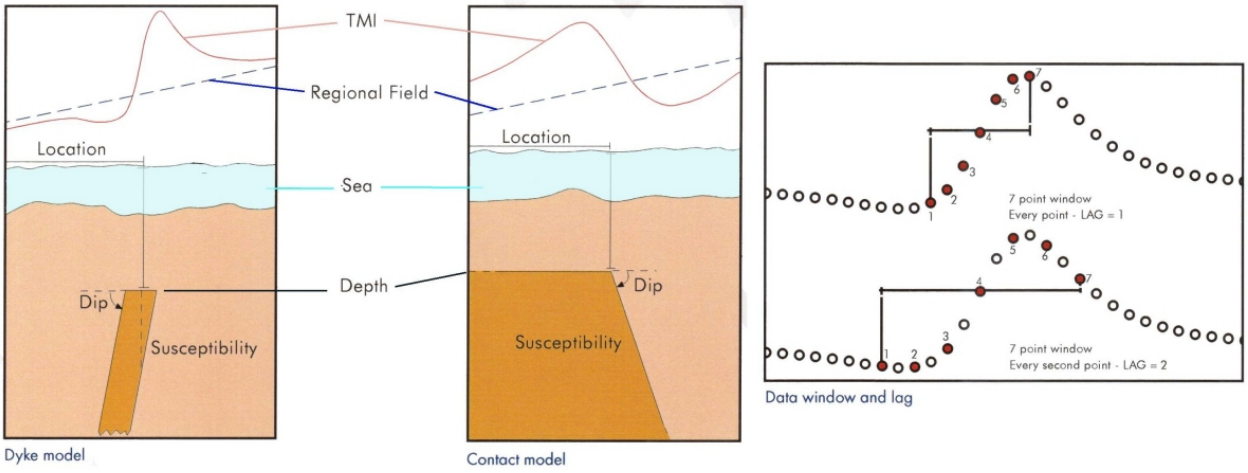

Figure 8-1: Schematic representation of the Werner parameters.

An extension of the method, using the First Horizontal Derivative, allows the same procedure to be performed for a contact-model geometry. Werner deconvolution is usually run on both the Horizontal Derivative and the Total Magnetic Intensity data to generate both contact and dyke solutions respectively.

The Werner deconvolution calculation routine utilised by the Geosoft Oasis montaj software is based on the USGS program PDEPTH (Phillips 1997) and includes an iterative improvement scheme described by Ku and Sharp (1983). Input profiles are interpolated to an even sample interval before the Werner processing, with the sample interval equal to the total profile length divided by the number of points in the profile.

The operator controls several parameters in the dialogue control which determines the number of solutions generated by the Werner deconvolution process. ‘Min. Window Length’ and ‘Max. Window Length’ set the minimum and maximum lengths of the Werner operator window. The ‘Window Expansion Increment’ is used to expand the Werner operator window length for successive passes from the ‘Min’ to the ‘Max’ whilst the ‘Window Shift Increment’ sets the

distance the Werner operator is moved along the profile between calculations. When setting these parameters it should be noted that the suggested optimum window length should be at least one half of the width of the anomalies being analysed (Ku and Sharp, 1983). It should also be noted that Werner deconvolution will not find many valid solutions at depths shallower than the input data interval or deeper than the window length.

As mentioned above, each Werner calculation potentially generates a solution. Initial solution selection is an automated process with two input parameters determining whether a solution will be saved. 'Residual cut-off' sets an amplitude threshold for anomalies below which anomalies are considered to be resultant from noise and are discarded. 'X cut-off' sets a horizontal distance threshold (as a percentage of the window length) for solutions relative to the centre of the Werner operator. Any solutions outside this distance will be discarded.

Werner deconvolution usually produces clusters of solutions around the 'real' solution resulting from multiple passes with differing window lengths. These clusters of solutions can be interactively collapsed into single, average solutions within the 'Pdepth' extension module (Figure 8-2). In addition, the solutions are compared with the profile and gridded magnetic data, and patterns and clustering of the solutions that are characteristic of particular types of geology can be identified. It is estimated that the calculated depths have an accuracy of approximately 90% in suitable circumstances.

The accuracy of Werner solutions is arguable subject matter. Generally, the solution accuracy depends on the following points:

- Discretion of the interpreter to pick valid solution clusters
- Model dependency (i.e. is the dyke/contact model valid)
- Considering model dependency, solution accuracy depends on the discretion of the interpreter to make the right choice in solution type, i.e. contact Vs dyke.
- Quality of data pre-processing
- Noise content of the data.
- The predominance of the targeted magnetic anomaly in the data (i.e. is the magnetic anomaly a superposition of anomalies from several sources)
- Orientation of sampled profiles
- Along profile sample spacing
- Werner input parameters

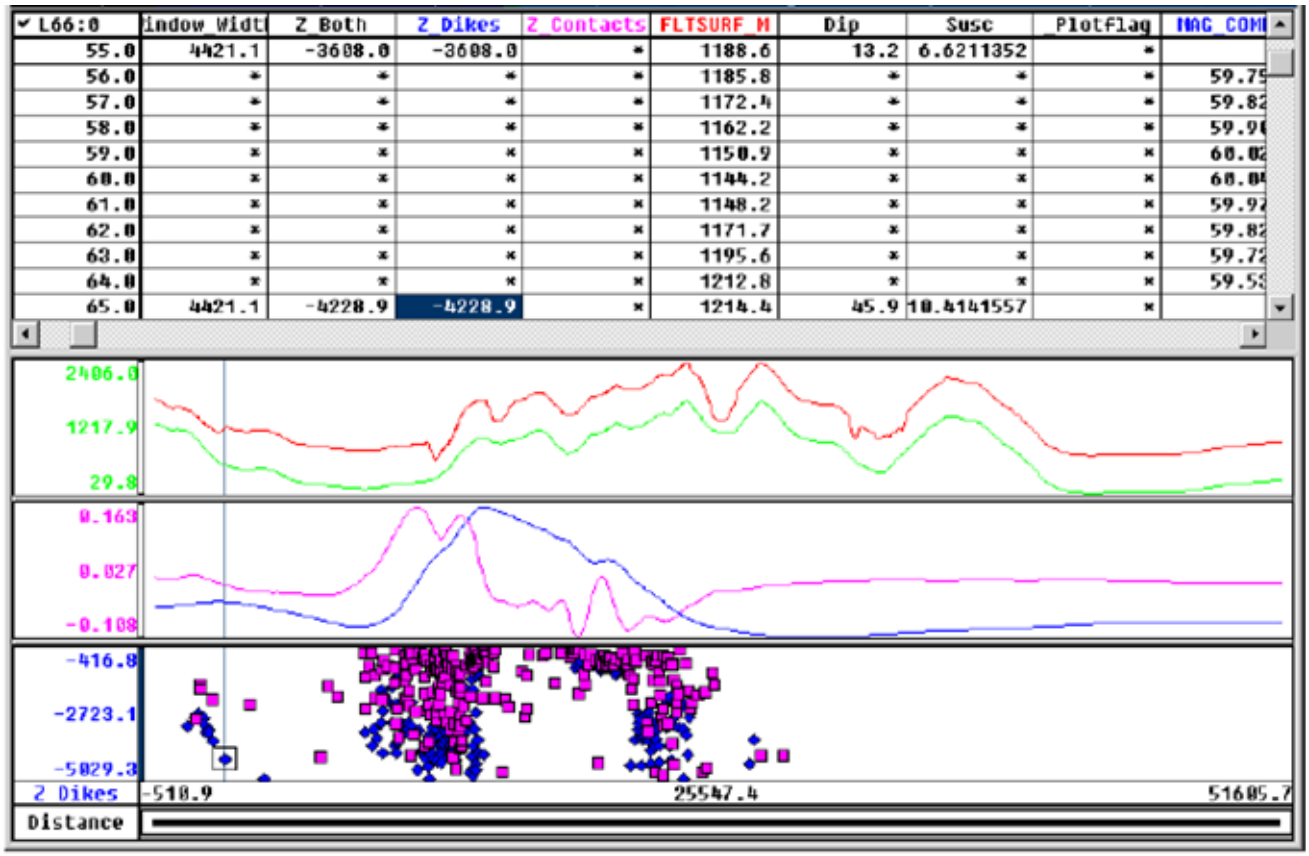

Figure 8-2: Werner solutions from Geosoft's Oasis montaj Pdepth extension module prior to clustering analysis. The database displays the various input channels as well as the Werner solutions ('Z_Dikes' and 'Z_Contacts' channels) which are plotted in the bottom panel. The middle panel (blue and magenta traces) displays the input magnetic profile and horizontal derivative whilst the top panel (red and green traces) shows the input flight elevation and topography respectively. It should be noted that the displayed susceptibilities are 'effective susceptibilities', that is the cgs susceptibility value multiplied by the dyke width.

8.2 PROFILE MODELLING AND INVERSION

The potential field measured at a point is dependent on the contrast between the relevant physical properties of a body and the background values. Consequently, the geophysical response from a pre-determined geological model can be calculated if assumptions are made about the physical properties and shape of the geological units. In practise, the response of a 2-dimensional geological model is compared with a profile of geophysical data taken from the same location. It is then possible to adjust the shape and physical properties of the units within the model within geologically realistic limits to obtain a better match between the measured and calculated profiles. It is apparent that construction of an infinite number of different models is possible to produce a calculated field to match the measured field. For potential field modelling to be meaningful, a reasonable idea of the expected geological formation must be available.

A number of software packages are available to undertake profile modelling and inversion. Packages such as 'Magmod3' and 'Potent' are relatively simple and can be used to generate preliminary models. In order to develop more complex multi-body models software such as Geosoft's 'GM-SYS' (formerly developed by Northwest Geophysical Associates, Inc.) or Encom's 'ModelVision Pro'. Each of these packages requires the development of a geological model with the simulated response compared with the field data.

From the initial interpretation of geophysical and complementary data, it is possible to generate theoretical "schematic" models that may account for the observed magnetic signatures. It is also possible to generate geological cross-sections that can be verified by modelling magnetic profiles. Initial models should include all available information, including preliminary geological cross-sections, depth estimation from Werner or Euler deconvolution, inversion of selected anomalies, estimates of contact positions from gradient maxima plots, borehole data, field measurements (eg. dip, strike, magnetic susceptibility) and seismic sections.

Parameters used in constructing a model of a geological body, such as dip, width and extent, are shown in Figure 8-3.

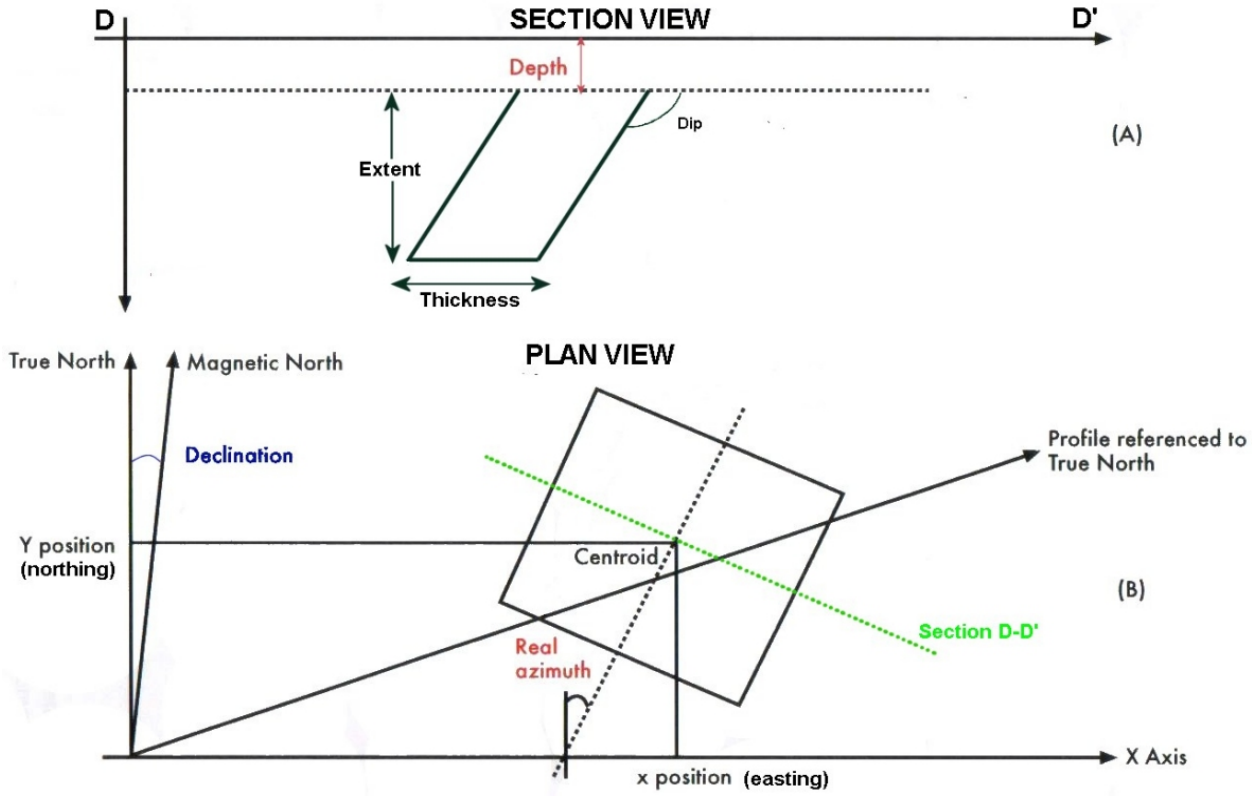

Figure 8-3: Modelling parameters (A) diagram displaying cross-section of model with depth parameter, (B) display of surface of model with length and azimuth.

Initial models can be adjusted both interactively and using inversion facilities within modelling software until a satisfactory fit is obtained between the observed and modelled data. These model cross-sections are then appraised for their geological validity and further changes incorporated into the next version of the model cross-section. This process can result in numerous iterations of the validation procedure before acceptable results are obtained.